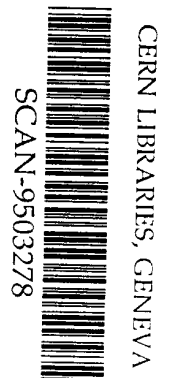


PT

# Physikalisch Technische Bundesanstalt



80 3514

---

Alexandru V. Alevra, Horst Klein and Ulrich J. Schrewe  
**Measurements with the PTB Bonner Sphere Spectrometer  
in High-Energy Neutron Calibration Fields at CERN**  
(CERN-CEC Experiment H6J93, July 1993)

PTB-N-22  
Braunschweig, December 1994

ISSN 0936-0492  
ISBN 3-89429-573-2

---

# **Physikalisch-Technische Bundesanstalt**

Neutronenphysik

PTB-Bericht N-22

**Measurements with the PTB Bonner Sphere Spectrometer  
in High-Energy Neutron Calibration Fields at CERN  
(CERN-CEC Experiment H6J93, July 1993)**

by

Alexandru V. Alevra, Horst Klein and Ulrich J. Schrewe

## C O N T E N T S

1. INTRODUCTION	1
2. THE FIELDS INVESTIGATED	1
3. THE PTB "C" BONNER SPHERE SPECTROMETER	4
4. THE MEASUREMENTS	6
5. RESULTS	9
5.1 The results obtained using the response matrix C-D_90.RES	11
5.2 The results obtained using the extended response matrix C-1_94.A61 and a limited a priori information	11
5.3 The results obtained using the response matrix C-1_94.A61 and a priori information from FLUKA calculations	12
6. DISCUSSION	16
7. ACKNOWLEDGEMENTS	17
8. REFERENCES	17
APPENDIX A: The fluence response matrices used in the data analysis and the Bonner sphere readings in the four measurement positions	19
APPENDIX B: The PTB-BS solutions (type "53E") for all four measurement positions using the fluence response matrix C-D_90.RES	23
APPENDIX C: The PTB-BS solutions (type "61E") for all four measurement positions using the fluence response matrix C-1_94.A61	29
APPENDIX D: The PTB-BS solutions (type "61X") for all four measurement positions using the fluence response matrix C-1_94.A61	35
APPENDIX E: The group values of the fluence and the dose equivalent for all four measurement positions and all solution types	41

**Abstract** — The PTB Bonner sphere spectrometer was used to measure neutron spectral fluences contributing to four mixed high-energy calibration fields produced at the CERN Super Proton Synchrotron. The results are compared with calculations.

**Resumé** — Le spectromètre multisphères du PTB a été utilisé pour mesurer les spectres des neutrons contribuant à quatre champs mixtes d'étalonnage haute énergie produits au Super Synchrotron de Protons de CERN. Les résultats sont comparés avec des calculs.

**Zusammenfassung** — Das Bonner-Kugel Spektrometer der PTB wurde am CERN eingesetzt, um die spektrale Neutronenfluenz in vier verschiedenen hochenergetischen gemischten Feldern, die am Super Proton Synchrotron für Kalibrierzwecke erzeugt wurden, zu bestimmen. Die Meßergebnisse werden mit Rechnungen verglichen.

## Die Serien der PTB-Berichte:

Atomphysik	PTB-APh
Dosimetrie	PTB-Dos
Elektrizität	PTB-E
Elektronische Entwicklung	PTB-EW
Fertigungsmeßtechnik	PTB-F
Informationstechnik	PTB-IT
Literaturzusammenstellungen und Veröffentlichungshinweise	PTB-L
Mechanik und Akustik	PTB-MA
Medizinische Meßtechnik	PTB-MM
Neutronenphysik	PTB-N
Internationale Organisation für Gesetzliches Meßwesen	PTB-OIML
Optik	PTB-Opt
Physikalische Grundlagen	PTB-PG
Radioaktivität	PTB-Ra
Technisch-Wissenschaftliche Dienste	PTB-TWD
Thermodynamik	PTB-W

## Ausgelaufene Serien:

Akustik	(bis 1985)	PTB-Ak
Forschungs- und Meßreaktor Braunschweig	(bis 1988)	PTB-FMRB
Institut Berlin	(bis 1985)	PTB-IB
Mechanik	(bis 1985)	PTB-Me
Neutronendosimetrie	(bis 1988)	PTB-ND
Sicherstellung und Endlagerung radioaktiver Abfälle	(bis 1989)	PTB-SE

---

**Herausgeber:** Physikalisch-Technische Bundesanstalt, Braunschweig und Berlin  
Referat Schrifttum, Telefon: (0531) 592-93 12

Bundesallee 100  
D-38116 Braunschweig  
Telefon: (0531) 592-0  
Telefax: (0531) 592-92 92  
Teletex: 5 31 82 09 PTB  
Telex: 95 28 22 ptd d

**Vertrieb:**  
Wirtschaftsverlag NW  
Verlag für neue Wissenschaften GmbH  
Am Alten Hafen 113-115  
D-27568 Bremerhaven  
Telefon: (0471) 460 93-95  
Telefax: (0471) 427 65

## 1. INTRODUCTION

Increased interest in the dosimetry, and by implication the spectrometry, of high-energy particle fields is due not only to radiation protection practice at high-energy (GeV+TeV) accelerators, which has become established, but also to the increasing use of the high-energy particles in cancer therapy and, last but not least, to the ICRP's acknowledgement of the occupational exposure of civil aircraft personnel during flights at high altitude [1].

In the complex stray radiation fields encountered outside the shields of high-energy accelerators, the neutron component is the major contributor to the dose equivalent, and for this reason particular attention is paid to neutron dosimetry in these fields. As the dose-equivalent responses of the present dosimeters depend on the neutron spectra, spectrometry is applied to determine the dose equivalent with acceptable accuracy, and so to establish a reference for other instruments.

Within the framework of a CERN - CEC project a series of measurements was performed in various high-energy radiation fields at CERN, and several European laboratories were invited to take part with spectrometers and dosimeters in these investigations. In one of these series which was carried out in July 1993, the PTB participated with the PTB "C" Bonner sphere spectrometer.

A comparison of the results obtained by all the participants will be published elsewhere. In the present paper the results obtained with the PTB Bonner spheres are reported.

## 2. THE FIELDS INVESTIGATED

The mixed high-energy radiation fields were produced using the beam of the CERN Super Proton Synchrotron (SPS) in the H6 beam line of the North Experimental Hall. The beam consisted of 205 GeV/c positively charged particles estimated to be a mixture of about 2/3 protons and 1/3 pions [2, 3].

As is usual for high-energy accelerators, the beam has a time structure which must be taken into account in order to avoid pulse pile-up and to properly correct the measured count rates for dead-time losses. The time structure of the CERN SPS "spills" is shown in Fig. 1.

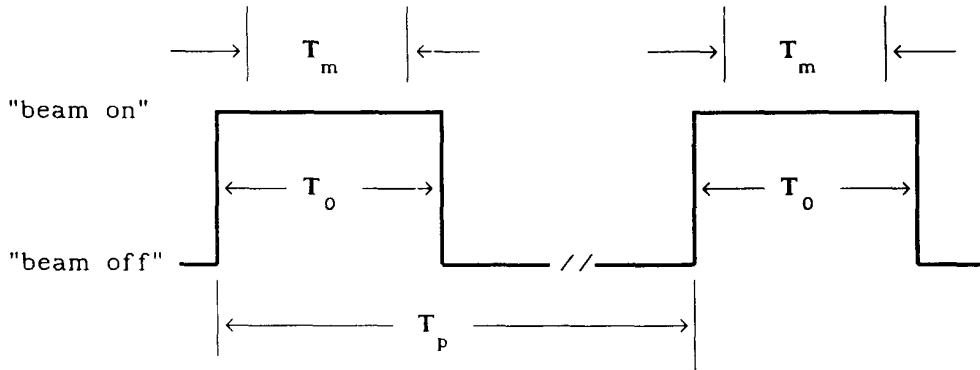


Fig. 1 The time structure of the CERN - SPS beam. The beam pulse length was  $T_0 = 2.3$  s and the beam pulse period was  $T_p = 14.4$  s. Measurements were performed during a gate period  $T_m = 1.7$  s.

The beam collided with a thick copper target (7 cm  $\emptyset$  x 50 cm), which was located alternatively in one of two shielding configurations specially prepared for this series of measurements. The shieldings and the measurement geometry are shown in Fig. 2 as taken from reference [2] and slightly modified in order to indicate the measurement positions chosen for the PTB Bonner spheres.

In one configuration the shielding around the target consisted of 80 cm concrete both at the side and on the top (see cut AA in Fig. 2). In the other configuration (see cut BB) the side shielding consisted of 160 cm concrete, while for the top shielding iron plates with a total thickness of 40 cm were used.

In order to establish fixed points for measurements, in each configuration the centre of the target was taken as reference and with respect to this point a grid of 16 cubic cells (numbered from 1 to 16) each with a side length of 50 cm was defined on the top shielding. The centres of these cells, placed 25 cm above the shielding, are the points of measurement for the various instruments. In a similar way a grid of 8 cubic cells (numbered from 1 to 8) of the same size and placed at the height of the beam close to the side shielding was defined. The four measurement positions of the PTB

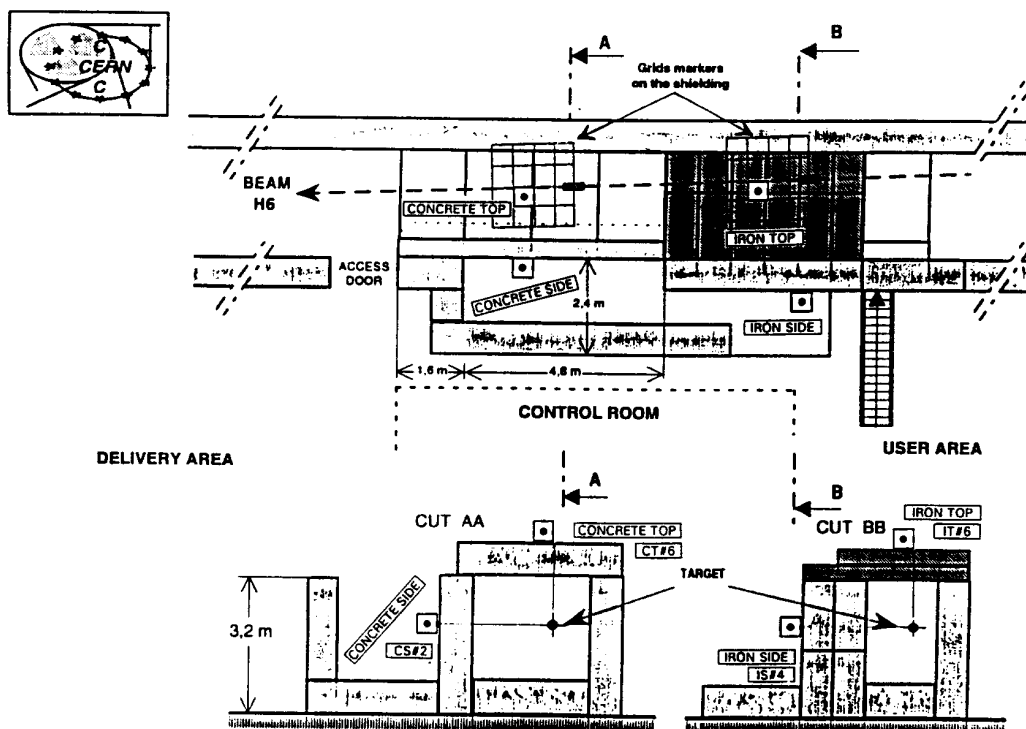


Fig. 2 The two shielding configurations and the measurement positions of the PTB Bonner spheres during the July 1993 series of measurements at CERN - SPS. The "iron side" position (IS#4) is also called "thick concrete" (TC#4).

Bonner spheres which coincide with those of other participants are indicated in Fig. 2 by squares with a point in their centre and listed in Table 1.

Table 1. The measurement positions of the PTB Bonner spheres.

Position	Cell	Short Names	Distance to Shielding	Downstream from Target
CONCRETE TOP	Nr.6	CT#6, CT	25 cm	125 cm
CONCRETE SIDE	Nr.2	CS#2, CS	25 cm	125 cm
IRON TOP	Nr.6	IT#6, IT	25 cm	125 cm
IRON SIDE	Nr.4	IS#4, IS	25 cm	25 cm

The neutron fields encountered in practice are usually accompanied by other radiations. It is typical of high energy accelerators that even in places protected by heavy shielding, not only neutrons and



photons but also secondary charged particles can be found. For the measurement geometry shown in Fig. 2, the neutron and charged hadron (protons and pions) components of the radiation fields have been calculated by Roesler and Stevenson using the FLUKA Monte Carlo code, the results being reported in Ref. 3. In relation to the neutron component, the mixed proton-pion contribution at various points of measurement is estimated to be 1% to 2.5% in fluence and 3% to 8% in dose equivalent. The highest values are obtained behind concrete shieldings, the lowest ones behind iron.

### 3. THE PTB "C" BONNER SPHERE SPECTROMETER

The spectrometer consists of twelve high-density ( $0.946 \text{ g/cm}^3$ ) polyethylene spheres with diameters ranging from 7.62 cm to 45.72 cm (3", 3.5", 4", 4.5", 5", 6", 7", 8", 10", 12", 15" and 18") having at their centre a spherical proportional counter ( $\emptyset$  3.2 cm) of type SP90, produced by Centronic Ltd, UK, filled with 200 kPa of  $^3\text{He}$ . The bare counter and occasionally the bare counter under a cadmium cover are also used as parts of the spectrometer.

The fluence responses of the spheres are based on experimental calibrations with monoenergetic neutrons from 1.17 keV to 14.8 MeV [4] and with thermal neutrons [5], using the energy-dependent responses calculated with the ANISN code [6] for interpolation and extrapolation purposes. The response matrix resulting for neutron energies from 1 meV to 25.12 MeV (C-D\_90.RES) is shown in Fig. 3 and given numerically in Table 3 of Appendix A. The estimated uncertainties of the response values (in terms of one standard deviation, as everywhere throughout this report) are also given in the table. They consist of an uncorrelated part which accounts for internal shape or height inconsistencies between the responses of various spheres, and a correlated part common to all sphere diameters in the entire energy range, reflecting the limitations due to the data basis used for the calculations and the fluence measuring method applied for the experimental calibrations. This correlated part must be quadratically added to all final results, differential or integral, expressed in terms of fluence or dose equivalent.

Although inadequate for the investigation of the whole neutron energy spectrum produced in the present experiment, the response

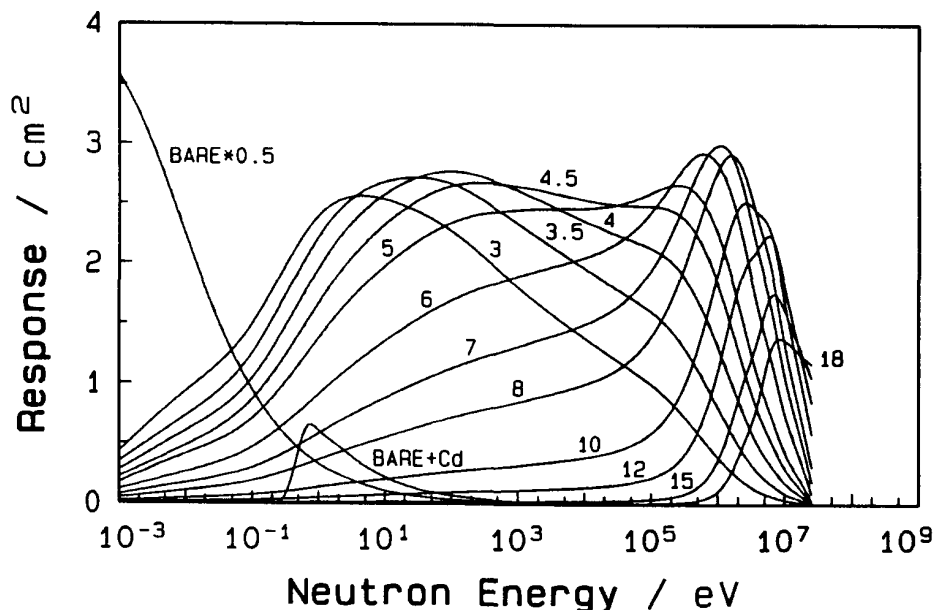


Fig. 3. The fluence responses of the PTB "C" Bonner spheres from thermal energies to 25.12 MeV (C-D\_90.RES).

matrix from Fig. 3 was used in the first series of data unfolding with the purpose of obtaining the partial neutron spectral fluence below about 10 MeV without using any *a priori* information on the spectra.

In order to make possible the investigation in the whole energy range covered in this experiment, the extension of the PTB response matrix up to a few hundred MeV became necessary. For this purpose, the high-energy part of different calculated responses found in the literature [7-9] were fitted to our responses in the energy range from 1 MeV to 10 MeV, and calibration measurements with 55.15 MeV neutrons [10] were performed at PSI Villigen / Switzerland to select the most appropriate extension to higher energies. Only the high-energy shapes of the IAR Lausanne response matrix [7], which extends up to 387.5 MeV, proved to be compatible with the 55.15 MeV calibrations. For sphere diameters of 3.5", 4", 4.5" and 7", contained in our BS set but not considered in Ref. 7, spline interpolations on sphere diameters have been performed. The high-energy response of the 18" sphere, also not found in Ref. 7, was guessed taking into account the regularities of shape of the other IAR response functions. Finally the responses obtained were empirically

extrapolated up to 1 GeV. The resulting extended "C" response matrix is shown in Fig. 4 and given numerically in Table 4 of Appendix A.

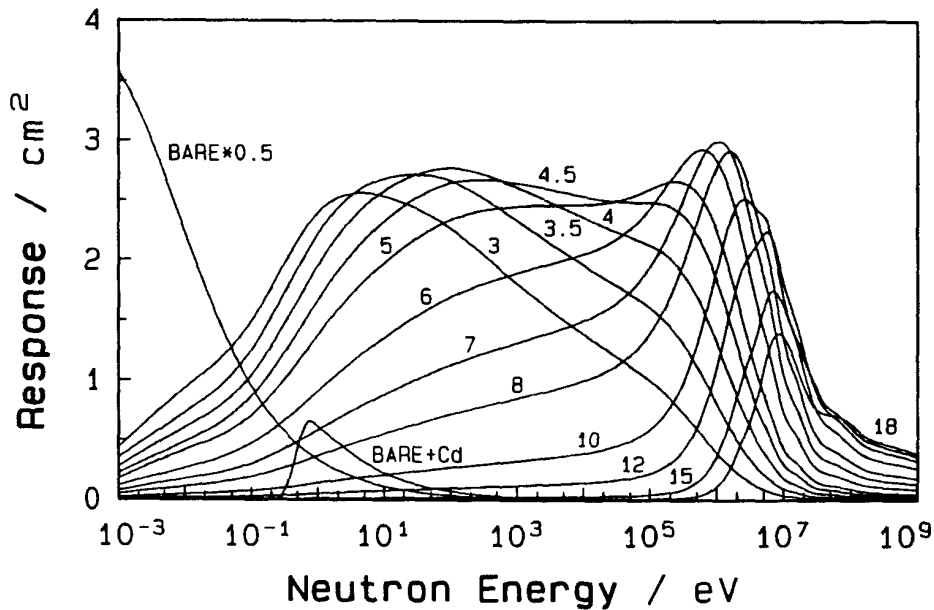


Fig. 4. The fluence responses of the PTB "C" Bonner spheres from thermal energies to 1 GeV (C-1\_94.A61).

The spectral fluence of the PSI Villigen *quasi-monoenergetic* neutron field of 55.15 MeV peak energy determined using this response matrix shows full agreement in shape with time-of-flight measurements ( $E_n > 5$  MeV, NE 213 scintillation detector) and agrees within  $\pm 8\%$  in absolute fluence with reference measurements using a solid-state proton-recoil telescope ( $E_n > 48$  MeV). The guessed 18" response is included in this result. The uncertainties given in Table 3 are the same as for the C-D\_90.RES response and are still valid for spectral fluences up to about 20 MeV. For higher-energy parts of a spectrum, a supplementary correlated uncertainty of  $\pm 10\%$  should be quadratically added to the final results.

#### 4. THE MEASUREMENTS

The beam monitoring was realized by means of a *Precision Ionisation Chamber* (PIC), used as transmission chamber in beam, one count of this instrument being estimated to correspond to  $2 \cdot 10^4$  particles incident on the target. All the results presented in this report were normalized to one PIC count.

In the Bonner sphere measurements, the pulses produced by the central detector were counted using electronics consisting of a preamplifier, an amplifier and a discriminator connected to a scaler, the entire system having a non-extending dead-time of  $4 \mu\text{s}$  per event. A dead-time correction is simple if the count rate is constant during the measurement. In order to fulfil this condition a time window of 1.7 s has been set in the beam-on periods (see Fig. 1) for the Bonner sphere counting and simultaneously applied to the PIC counter. A maximum count rate of the order of  $7 \cdot 10^3 \text{ s}^{-1}$  was attained in this measurement series by the 5" sphere in the IT#6 position, where the dead-time correction amounted to 2.7%. The PIC count rates were not corrected for dead-time, but they were almost the same during the BS measurements at a certain point.

The Bonner spheres equipped with a  $^3\text{He}$ -filled proportional counter have the advantage of being sensitive practically only to neutrons. Nevertheless, in order to ensure that noise or gamma-ray induced events were not included in the reading, the pulse-height spectra from the central counter were measured simultaneously. The pulse-height spectrum taken during the measurement with the 8" sphere in the CT#6 position is shown as an example in Fig. 5. The spectra from all other measurements reported here are similar, at least as far as it is possible to clearly distinguish the pulses induced by neutrons from those due to noise and photon events. In

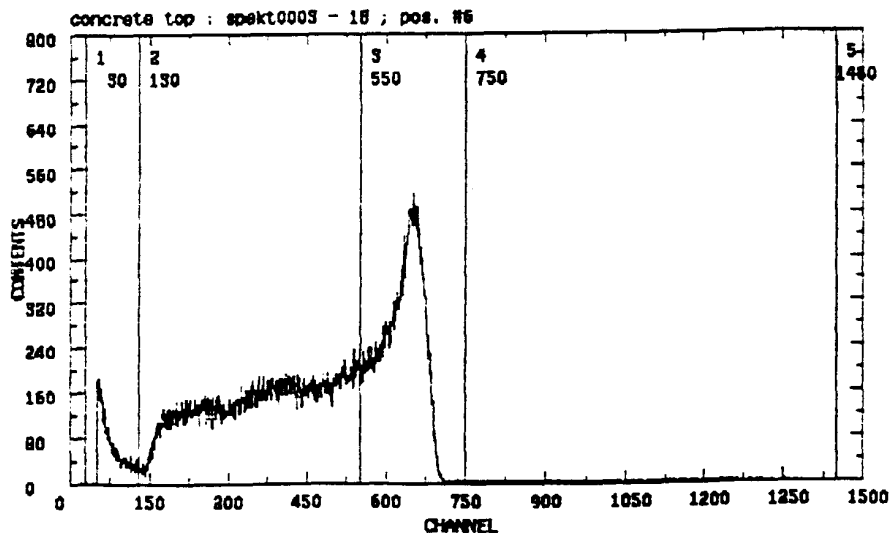


Fig. 5. The pulse-height spectrum obtained from the central detector during the measurement with the 8" sphere in the CT#6 position.

Fig. 5 the pulses with amplitudes higher than channel 130 were attributed to neutrons, those of lower amplitude to photon-induced events and noise. Pulses with amplitudes higher than channel 750 are chiefly due to the pile-up of neutron events (the count rate was about 1800 pulses per second) and they were included in the readings.

The influence of the secondary charged hadron components present in the investigated mixed-fields on the BS count rates was not evaluated and was therefore not separated from the contribution of the high-energy neutrons. The nuclear interactions of the high-energy protons and pions, which amount to 1% to 2.5% in fluence compared with the neutrons (see section 2 of this report), in the polyethylene of the spheres are similar to those of the high-energy neutrons, at least with regard to the production of secondary neutrons that have a chance of being thermalized and detected. For this reason the results expressed in terms of spectral neutron fluence should be interpreted as including in their high-energy part (from a few tens of MeV) a certain fraction of the 1% to 2.5% mixed proton-pion fluence.

The readings corrected for dead-time losses and normalized to one PIC count are listed in Table 5 of Appendix A, together with their statistical uncertainties and the uncorrelated uncertainties attributed to the fluence responses. The readings obtained with a Leake-type REM counter normalized in the same way are also given in this table.

The stability of the monitor and the Bonner spheres during the whole period of measurement can be judged from the representation of the BS readings (relative to the 5" sphere reading) as a function of the sphere diameter. These are shown for all four PTB measurement positions in Fig. 6 (a to d). The smoothness of the curves indicates the good stability of all instruments involved in the four series of measurements. The curves presented generally differ in shape, but those obtained near the concrete shielding (a and b) are very similar. As large-diameter spheres and the bare counter as well show rather large readings, considerable contributions to the spectrum are expected in both the high-energy and thermal regions. But above the iron shield (curve c) these contributions appear to be lower.

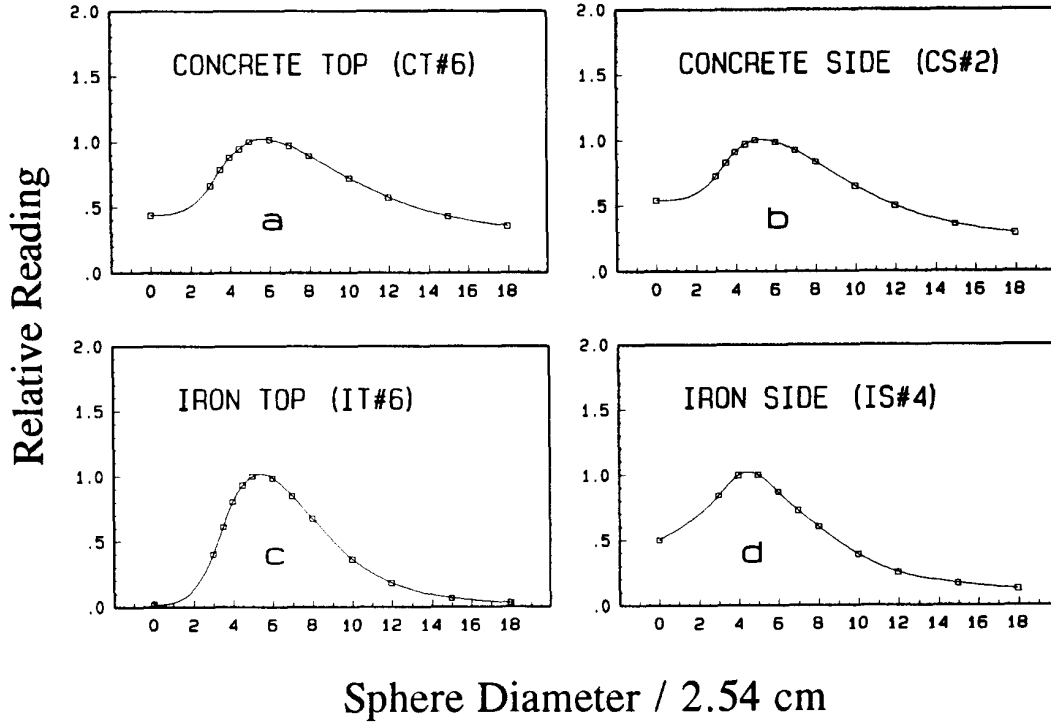


Fig. 6. The relative readings of the PTB Bonner spheres as a function of the sphere diameter for the four measurement positions.

## 5. RESULTS

For the *few-channel* unfolding of the measured BS data a *home-made* program based on the SAND-II algorithm [11] was used. As usual in this kind of unfolding, the solution is not unique and depends on the shape of the guess spectrum given in the input. During the unfolding a small number of iterations (usually no more than 10) are allowed and the changes in shape due to the first few iterations are observed. These changes are used as indications of the way in which the guess spectrum should be modified.

Assuming a solution spectrum,  $\Phi^s$ , we can simulate our BS readings for this spectrum calculating

$$C_d^s = \sum_{i=1}^{n_E} R_{d,i} \cdot \Phi_i^s \quad (d = 1, 2, \dots, n_D) \quad (1)$$

where  $n_E$  is the number of energy bins in which we describe the spectrum,  $n_D$  is the number of BS's used,  $R_{d,i}$  is the fluence response of the  $d$ -th BS in the  $i$ -th energy bin, and  $\Phi_i^s$  is the solution fluence in the same bin.

Using these calculated readings and the measured readings

$$M_d \quad (d = 1, 2, \dots, n_D)$$

we can construct the reading ratios

$$r_d^s = \frac{M_d}{C_d^s} \quad (d = 1, 2, \dots, n_D) \quad (2)$$

and obtain their relative uncertainties from

$$\sigma_{\text{rel}}^2(r_d^s) = \sigma_{\text{rel}}^2(M_d) + \sigma_{\text{rel}}^2(C_d^s) \quad (3)$$

where  $\sigma_{\text{rel}}(M_d)$  is the relative statistical uncertainty of the reading (statistical of BS and monitor readings) as given in Table 5 of Appendix A, and  $\sigma_{\text{rel}}(C_d^s)$  is considered to consist only of the uncorrelated relative uncertainty of the response, also given in Table 5.

The weighted mean value of the ratios  $r_d^s$  is obtained from

$$\langle r_d^s \rangle = \frac{\sum_{d=1}^{n_D} r_d^s \cdot w_d}{\sum_{d=1}^{n_D} w_d} = \frac{\sum_{d=1}^{n_D} r_d^s / \sigma^2(r_d^s)}{\sum_{d=1}^{n_D} 1 / \sigma^2(r_d^s)} \quad (4)$$

the weights being the inverses of the variances of  $r_d^s$

$$w_d = 1 / \sigma^2(r_d^s) \quad (5)$$

where  $\sigma(r_d^s)$  is the absolute standard deviations of  $r_d^s$ .

The absolute standard deviation of  $\langle r_d^s \rangle$  is obtained from

$$\sigma^2(\langle r_d^s \rangle) = \frac{1}{\sum_{d=1}^{n_D} 1 / \sigma^2(r_d^s)} \quad (6)$$

The spread of the individual  $r_d^s$  values about their mean  $\langle r_d^s \rangle$  is well described by the value of the *reduced chi-squared*:

$$\chi_r^2 = \frac{1}{n_D - 1} \sum_{d=1}^{n_D} \frac{[\langle r_d^s \rangle - r_d^s]^2}{\sigma^2(r_d^s)} \quad (7)$$

A solution spectrum,  $\Phi^s$ , is considered valid if it is physically appropriate and produces  $r_d^s$  values so that  $\langle r_d^s \rangle$  is very close to unity and their spread about unity is compatible with the statistics. As one *standard deviation*,  $\sigma(r_d^s)$ , corresponds to a 68% confidence interval and we have used  $n_D = 13$  detectors in this work,

i.e. 12 spheres and the bare counter, this means that for a valid solution at least nine  $r_d^s$  values will deviate from unity by less than one standard deviation, and the others will not deviate by more than  $2 \cdot \sigma(r_d^s)$ . In this case the value of the *reduced chi-squared* will lie close to unity or even lower.

Various results are presented numerically and graphically in Appendices B to D. In the upper part of each figure the solution spectrum is shown as a histogram, while in the lower part the ratios *measured / calculated* readings of the various BS's,  $r_d^s$ , are represented. The uncertainty bar on the left side of a point indicates the relative uncertainty of the measured reading,  $\sigma(M_d)$ , the bar on the right indicating the uncertainty  $\sigma(r_d^s)$ .

### 5.1 The results obtained using the response matrix C-D\_90.RES

The unfolding of the measured data was done in this case without any use of *a priori information*. This means that a large variety of spectral shapes were produced and used as *guess input spectra* until an adequate shape was found. In constructing the *guess input spectra* the neutrons with energies higher than 12.59 MeV were concentrated in the last two bins covering the energy interval from 12.59 MeV to 31.62 MeV. As beyond this interval the BS responses are not constant but decrease with increasing energy, it is obvious that the "high-energy" fluence which is obtained underestimates the reality. On the other hand, the unfolding for neutron energies below 12.59 MeV can be done almost independently of the high-energy reality, the quality of the result being unaffected by the larger uncertainties of the response matrix at high energies.

The solutions obtained from this kind of unfolding (file names with the extension "53E") for all four measurement positions are presented in Appendix B and also shown in Fig. 7 as dot-dot-dashed curves.

### 5.2 The results obtained using the extended response matrix C-1\_94.A61 and a limited a priori information

With the response matrix C-1\_94.A61, solution spectra extending up to 1 GeV can be produced. Unfortunately, for neutron energies higher



than about 50 MeV, although different in magnitude the response functions of various spheres are very similar in shape and on account of that the spectrometric ability of the BS's becomes extremely poor. In this case the use of some *a priori information* is obligatory.

Taking into account the way the neutrons are produced and the shielding configurations in this series of measurements, it can be expected that the high-energy part of the spectrum mainly consists of neutrons produced by spallation reactions. In order to approach a spallation spectrum, a Maxwellian distribution with the maximum at about 80 MeV was introduced in all *guess* spectra and the amount of this contribution was carefully determined in each case by unfolding.

The solutions obtained from this kind of unfolding (file names with the extension "61E") are presented in Appendix C and also shown in Fig. 7 as smooth full curves.

### 5.3 The results obtained using the response matrix C-1\_94.A61 and *a priori* information from FLUKA calculations

As neutron spectra calculated for the same geometries as investigated with our BS's became available [3], these could be used as *a priori information* in the *input guess spectra*. For this purpose the calculated spectra, which are normalized to one incident charged particle (proton or pion), were renormalized to one PIC count (i.e. multiplied by  $2 \cdot 10^4$  incident particles / PIC count) and rebinned to match the description of our data in 61 energy groups logarithmically equidistant, 5 per decade (see matrix C-1\_94.A61 in Appendix A and numerical data listed in Appendices C and D). In constructing the guess spectra we took a mixture of 2/3 proton- and 1/3 pion-induced calculated spectra. These mixed calculated spectra, renormalized to one PIC count but still in their original energy binning, are shown in Fig. 7 as discrete points whose uncertainty bars indicate the statistical uncertainties from the Monte Carlo calculations.

From Fig. 7 it can be seen that the calculations fail to describe completely the low-energy part of the spectra (the lowest energy in

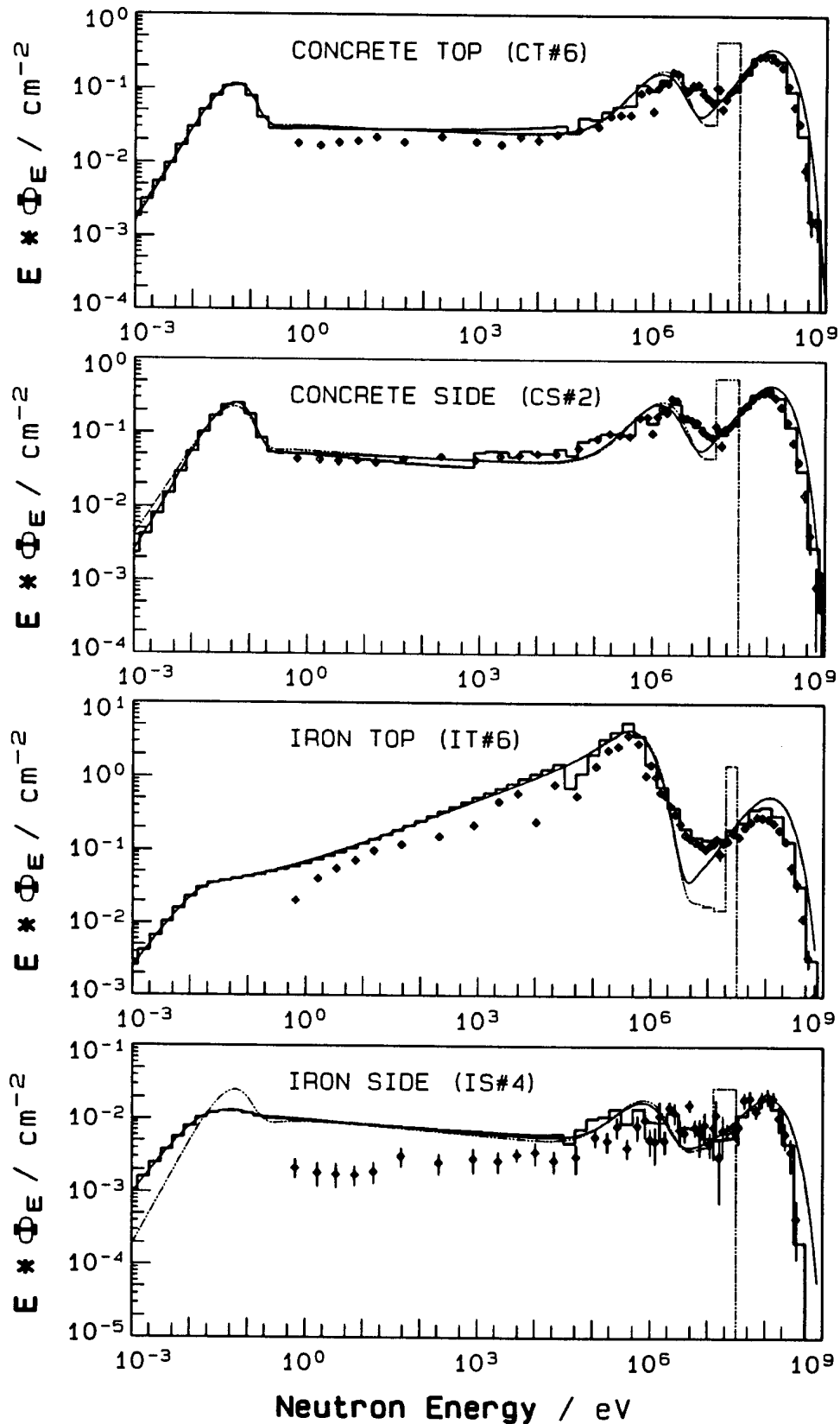


Fig. 7. The various BS solution spectra (53E: dot-dot-dashed curve; 61E: smooth full curve; 61X: histogram) compared with calculations (points). See more explanations in text.

calculations is 0.5 eV). For this reason only calculated results for neutron energies higher than about 10 keV were introduced in the *input guess* spectra, the rest being taken from our "53E"-type solutions.

The solutions obtained from this kind of unfolding (file names with the extension "61X") for all four measurement positions are presented in Appendix D and also shown in Fig. 7 as histograms.

Fig. 7 allow a qualitative comparison to be made of different types of BS solutions together with the calculations.

For quantitative comparisons the integral data of interest were calculated and are given together with the spectra in Appendices B to D, or systematized for all solution spectra in the tables given in Appendix E. The reported values refer to the neutron fluence and dose equivalent integrated over the whole energy range from 1 meV to 1 GeV, or over four adjacent energy groups with the limits at 1 meV, 0.4 eV, 10 keV, 10 MeV and 1 GeV.

The dose equivalent values reported in this work are:

- $H_{21} = \sum h_{21}(E_i) \cdot \Phi_i$ , where  $h_{21}$  is the fluence-to-dose conversion function according to ICRP 21 [12].
- $H_{39} = \sum h_{39}(E_i) \cdot \Phi_i$ , where  $h_{39}$  is the fluence-to-ambient-dose conversion function (i.e.  $H^*(10)/\Phi$ ) according to ICRU 39 [13,14].
- $H_{60G} = \sum h_{60G}(E_i) \cdot \Phi_i$ , where  $h_{60G}$  is the fluence-to-ambient-dose conversion function (i.e.  $H^*(10)/\Phi$ ) according to ICRP 60 [1,15].

The integral values  $H_{21}$ ,  $H_{39}$  and  $H_{60G}$  resulting from the BS spectral solutions of type "61X" are given in Table 2 for all four measurement positions. The uncertainties of these results were obtained taking into account a 15 % uncertainty of the dose equivalent produced by neutrons with energies below 10 MeV, and a 35 % uncertainty of the dose equivalent produced by higher-energy neutrons. For comparison, the results we obtained with the Leake-REM counter (calibrated with a bare  $^{252}\text{Cf}$  neutron source) and those obtained with the CERN-HANDI TEPC and reported in Ref. 16 are also listed in Table 2, in absolute values and, in the last two columns of the table, relative to the BS results. It should be noted (the measurement positions for HANDI are indicated in column four) that the TEPC measurements in "SIDE" positions are spatially slightly

Table 2. The dose equivalent values obtained in the four measurement positions with the PTB Bonner spheres, with the Leake-type REM counter and with the CERN HANDI-type TEPC\*).

The dose equivalent is given in pSv/PIC-count :

1) C93-CT.DOS → CERN (24.07.93) - CONCRETE TOP POS#6

	PTB-C-BS	PTB-7.22-LEAKE	AHS-HANDI-POS#6	L/BS	H/BS
H21	448 ± 28%	220 ± 75%	436	0.49	0.97
H39	526 ± 29%	223 ± 75%		0.42	
H60G	534 ± 28%	281 ± 75%	501	0.53	0.94

2) C93-CS.DOS → CERN (24.07.93) - CONCRETE SIDE POS#2

	PTB-C-BS	PTB-7.22-LEAKE	AHS-HANDI-POS#3	L/BS	H/BS
H21	611 ± 28%	317 ± 75%	587	0.52	0.96
H39	714 ± 29%	321 ± 75%		0.45	
H60G	734 ± 27%	404 ± 75%	679	0.55	0.93

3) C93-IT.DOS → CERN (25.07.93) - IRON TOP POS#6

	PTB-C-BS	PTB-7.22-LEAKE	AHS-HANDI-POS#6	L/BS	H/BS
H21	2254 ± 19%	2817 ± 75%	1652	1.25	0.73
H39	2678 ± 19%	2855 ± 75%		1.07	
H60G	3629 ± 18%	3592 ± 75%	2324	0.99	0.64

4) C93-IS.DOS → CERN (25.07.93) - IRON SIDE POS#4 (THICK CONCRETE)

	PTB-C-BS	PTB-7.22-LEAKE	AHS-HANDI-POS#3	L/BS	H/BS
H21	32 ± 28%	22 ± 75%	44	0.69	1.38
H39	37 ± 27%	22 ± 75%		0.59	
H60G	40 ± 25%	28 ± 75%	50	0.70	1.25

\*) The AHS-HANDI results are taken from Ref. 16.

shifted in relation to the Bonner spheres. In the "CS" measurement HANDI was placed 50 cm upstream and in the "IS" measurement 50 cm downstream compared with the BS's. Taking into account the thickness of the shieldings, the results still bear comparison.

## 6. DISCUSSION

The PTB Bonner sphere best solutions for the four fields (measurement positions) investigated in the H6J93-CERN-CEC experiment are considered to be the "61X" type spectra because they were produced using the best available *a priori information* at high energies, namely fluence spectral distributions obtained from Monte Carlo simulations of the experiment [3]. They are taken as reference in the following.

Fig. 7 and Table 10a (Appendix E) indicate that both the "53E" and "61E" solution types agree within a few percent with the reference for neutron energies below 10 MeV. Above 10 MeV, as expected, the solutions of type "53E" underestimate the fluence in all four measurement positions by 21% to 33%, but solutions of type "61E", on the contrary, overestimate the fluence in the same energy region by 22% to 35%. This is obviously due to the fact that the spallation spectrum was placed higher in energy than that which resulted from the FLUKA Monte Carlo calculations.

Comparing the spectra from Monte Carlo calculations with the reference one should rather consider the neutron energies above 10 keV. In this case the shapes of the spectra are fully confirmed by the BS measurements and even for the absolute fluence values the agreement is good in both CONCRETE positions (less than 8% discrepancy). For the IRON SIDE position (IS#4) the FLUKA result is lower by 14% in absolute fluence than our reference. A large discrepancy is seen for the IRON TOP position (IT#6) where the FLUKA result is lower by 34%. It turns out that this spectrum is much softer than all the others (mean energy 5.3 MeV compared with 37 MeV, 31 MeV and 15 MeV in the other positions), and it could be that the FLUKA code encounters some difficulties in such cases.

Table 2 indicates very good agreement of the TEPC dose equivalent measurements with the Bonner spheres in both CONCRETE geometries, a

tolerable overestimation in the IS#4 position, but about 30% underestimation of the dose equivalent in the IT#6 position, where the *softest* spectrum was obtained. The results obtained with the Leake REM counter, which was calibrated with a bare californium source (mean energy 2.13 MeV), are not surprising. They clearly underestimate the dose equivalent in all *hard-spectra* fields and agree with the BS's only in the *soft* field IT#6.

## 7. ACKNOWLEDGEMENTS

The authors are indebted to Dr. M. Höfert and his staff at CERN for the excellent working conditions and efficient organisation of the comparison exercise, and to Dr. G.R. Stevenson who made available the numerical results from the Monte Carlo calculations of the neutron spectra reported in Ref. 3.

This work was partially funded by the Commission of the European Communities, Brussels, under contract No. FI3P-CT92-0002.

## 8. REFERENCES

- [1] ICRP Publication 60: *Recommendations of the International Commission on Radiological Protection*, Annals of ICRP, Oxford, Pergamon, 1991.
- [2] A. Aroua, M. Höfert and T. Buchillier: *First Results of the CERN-CEC July 1993 Experiment (H6J93)*, CERN/TIS-RP/TM/93-30 (Aug. 1993)
- [3] Stefan Roesler and Graham R. Stevenson: *July 1993 CERN-CEC Experiments: Calculation of Hadron Energy Spectra from Track-Length Distributions using FLUKA*, CERN/TIS-RP/IR/93-47 (November 1993).
- [4] Alevra, A.V., Cosack, M., Hunt, J.B., Thomas, D.J. and Schraube, H.: *Experimental Determination of the Response of four Bonner Sphere sets to Monoenergetic Neutrons (II)*, Radiat. Prot. Dosim. **40**, 91-122 (1992).
- [5] Thomas, D.J., Alevra, A.V., Hunt, J.B., and Schraube, H.: *Experimental Determination of the Response of four Bonner Sphere sets to Thermal Neutrons*, Radiat. Prot. Dosim. **54** (1), 25-31 (1994).
- [6] Thomas, D.J.: *Use of the Program ANISN to Calculate Response Functions for a Bonner Sphere Set with a  $^3\text{He}$  Detector*, Report RSA(EXT)31, National Physical Laboratory, Teddington, (UK), 1992.

- [7] Aroua, A., Grecescu, M., Lanfranchi, M., Lerch, P., Prêtre, S. and Valley, J.-F.: *Evaluation and Test of the Response Matrix of a Multisphere Neutron Spectrometer in a Wide Energy Range. Part II. Simulation*, Nucl. Instr. and Meth. **A321**, 305-311 (1992).
- [8] Sanna, R.S.: *Thirty-one Group Response Matrices for the Multisphere Neutron Spectrometer over the Energy Range Thermal to 400 MeV*, USAEC, HASL-267, (March 1973).  
also in :  
Awschalom, M. and Sanna, R.S. : *Applications of Bonner Spheres Detectors in Neutron Field Dosimetry*, Radiat. Prot. Dosim. **10**, 88-101 (1985).
- [9] Mares, V. and Schraube, H. : *Evaluation of the Response Matrix of a Bonner Sphere Spectrometer with LiI Detector from Thermal Energy to 100 MeV*, Nucl. Instr. and Meth. Phys. Res. **A337**, 461-473 (1994).
- [10] Alevra, A.V. and Schrewe, U.: *Measurements with the PTB "C" Bonner Sphere Spectrometer in the PSI Villigen 55 MeV Neutron Field for Spectrometric and Calibration Purposes*, PTB Report, to be published.
- [11] McElroy, W.N., Berg, S., Crockett, T. and Hawkins, R.G. : *SAND-II, a Computer- Automated Iterative Method for Neutron Flux Spectra Determination by Foil Activation*, Report AFWL-TR-67-41., U.S. Air Force Weapons Laboratory (1967).
- [12] ICRP Publication 21: *Data for Protection against Ionizing Radiation from External Sources*, Pergamon Press, New York, 1973.
- [13] ICRU Report 39: *Determination of Dose Equivalent Resulting from External Radiation Sources*, ICRU Publications, Bethesda, 1985.
- [14] Wagner, S., Großwendt, B., Harvey, I.R., Mill, A.J., Selbach, H.J. and Siebert, B.R.L., *Unified Conversion Function for the New ICRU Operational Radiation Protection Quantities*, Radiat. Prot. Dosim. **12**, 231-235 (1985).
- [15] Leuthold, G., Mares, V. and Schraube, H.: *Calculation of the Neutron Ambient Dose Equivalent on the Basis of the ICRP Revised Quality Factors*, Radiat. Prot. Dosim. **40**, 77-84 (1992).
- [16] Aroua, A., Höfert, M. and Sannikov A.V.: *HANDI-TEPC Results of the CERN-CEC July and September 1993 Experiments (H6J93, H6S93)*, Report CERN/TIS-RP/IR/93-45, October 1993.

## APPENDIX A

**THE FLUENCE RESPONSE MATRICES USED IN THE DATA ANALYSIS AND  
THE BONNER SPHERE READINGS IN THE FOUR MEASUREMENT POSITIONS**

**Explanations to Tables 3 and 4:**

**Table 3. The response matrix C-D\_90.RES (1 meV ÷ 25 MeV).**

**Table 4. The extended response matrix C-1\_94.A61 (1 meV ÷ 1 GeV).**

- The neutron energies,  $E_n$ , are given in eV.
- The fluence responses are given in  $\text{cm}^2$  [counts/(neutron/ $\text{cm}^2$ )].
- OCO, 3CO, 3C5, .... 12C indicate the bare counter, the 3" sphere, the 3.5" sphere, .... the 12" sphere, etc. cOCO indicates the cadmium-covered bare counter, while cRAT indicates the ratio  $\text{cRAT}(E_n) = R_{\text{cOCO}}(E_n) / R_{\text{OCO}}(E_n)$ .
- The uncertainties given at the lower part of the tables are estimated in terms of one standard deviation. They consist of an uncorrelated part ( $\sigma_{\text{uncorr}}$ ) which accounts for internal shape or height inconsistencies between responses of various spheres, and a correlated part ( $\sigma_{\text{corr}}$ ), common to all sphere diameters in the entire energy range, reflecting the limitations due to the data basis used for the calculations and the fluence measuring method applied for the experimental calibrations.

**Explanations to Table 5:**

**Table 5. The readings of the PTB-"C" Bonner spheres and their uncertainties in the four points of measurement.**

- The dead-time corrected readings are given relative to one PIC (Precision Ionisation Chamber) count.
- The uncertainties of the readings, always in terms of one standard deviation, contain the statistical uncertainties of the Bonner sphere counts and of the PIC counts. The uncertainties of the LEAKE rem counter readings have the same meaning.
- The last column in Table 5 gives the uncorrelated uncertainties of the "C" responses, i.e. the same as the  $\sigma_{\text{uncorr}}$  from Tables 3 and 4. The large uncertainty of 75% given in this column for the Leake rem counter does not refer to the fluence response of this instrument, but to its capability to predict the dose equivalent in an unknown neutron field which might differ considerably in spectral shape from the field in which the instrument was calibrated.







Table 5. The readings of the PTB-"C" Bonner spheres and their uncertainties in the four points of measurement.

		C93-CT.DAT				C93-CS.DAT				C93-IT.DAT				C93-IS.DAT							
		CERN - 1993 - CONCRETE TOP POS#6 (24.07.93)				CERN - 1993 - CONCRETE SIDE POS#2 (24.07.93)				CERN - 1993 - IRON TOP POS#6 (25.07.93)				CERN - 1993 - IRON SIDE POS#4 (25.07.93) (THICK CONCRETE)							
iD	Det	Reading (count/PIC-count)				Reading (count/PIC-count)				Reading (count/PIC-count)				Reading (count/PIC-count)				St.Dev.of Response			
1	0C0	8.053E-01 ± 0.756 %				1.611E+00 ± 0.500 %				7.001E-01 ± 1.615 %				1.673E-01 ± 2.792 %				2.900 %			
2	c0C0	1.225E+00 ± 0.558 %				2.165E+00 ± 0.534 %				1.586E+01 ± 1.202 %				2.808E-01 ± 0.955 %				2.000 %			
3	3C0	1.447E+00 ± 0.648 %				2.466E+00 ± 0.570 %				2.415E+01 ± 1.135 %				3.327E-01 ± 0.859 %				1.900 %			
4	3C5	1.621E+00 ± 0.517 %				2.715E+00 ± 0.507 %				3.159E+01 ± 0.989 %				3.327E-01 ± 0.859 %				1.800 %			
5	4C0	1.740E+00 ± 0.543 %				2.890E+00 ± 0.521 %				3.663E+01 ± 1.088 %				3.335E-01 ± 0.839 %				1.700 %			
6	4C5	1.837E+00 ± 0.497 %				2.975E+00 ± 0.477 %				3.931E+01 ± 1.008 %				2.900E-01 ± 1.238 %				1.200 %			
7	5C0	1.869E+00 ± 0.417 %				2.937E+00 ± 0.447 %				3.885E+01 ± 1.047 %				2.424E-01 ± 1.354 %				1.400 %			
8	6C0	1.783E+00 ± 0.587 %				2.752E+00 ± 0.502 %				3.341E+01 ± 1.077 %				2.014E-01 ± 1.005 %				1.300 %			
9	7C0	1.641E+00 ± 0.362 %				2.491E+00 ± 0.520 %				2.663E+01 ± 1.130 %				2.014E-01 ± 1.005 %				1.300 %			
10	8C0	1.328E+00 ± 0.519 %				1.931E+00 ± 0.590 %				1.431E+01 ± 1.138 %				1.298E-01 ± 1.014 %				1.300 %			
11	10C	1.055E+00 ± 0.576 %				1.486E+00 ± 0.547 %				7.180E+00 ± 1.157 %				0.839E-01 ± 1.472 %				1.600 %			
12	12C	7.886E-01 ± 0.626 %				1.066E+00 ± 0.539 %				2.683E+00 ± 1.186 %				0.559E-01 ± 1.839 %				2.000 %			
13	15C	6.510E-01 ± 0.650 %				8.580E-01 ± 0.606 %				1.316E+00 ± 1.367 %				0.416E-01 ± 1.154 %				3.000 %			
14	18C	2.020E-01 ± 0.882 %				2.905E-01 ± 0.914 %				2.584E+00 ± 1.184 %				0.201E-01 ± 2.207 %				75.000 %			

## APPENDIX B

THE PTB-BS SOLUTIONS (TYPE "53E") FOR ALL FOUR MEASUREMENT  
POSITIONS USING THE FLUENCE RESPONSE MATRIX C-D\_90.RES.

All the data are given per PIC count !

In constructing the *input spectra* no external *a priori* information was used. The neutrons with energies higher than 12.59 MeV were concentrated in the last two bins covering the energy interval from 12.59 MeV to 31.62 MeV.

**Explanations to the upper part of a figure:**

- The solution spectrum is plotted as a histogram. In order to get the spectrum in absolute values per PIC count, the plotted values must be multiplied by the factor given in the upper right part of the figure.

- F is the integral fluence in  $\text{cm}^{-2}$ .

- H21, H39 and H60G are the integral dose equivalent according to ICRP21, ICRU39 and ICRP60, respectively, in Sv (see Section 5.3).

-  $E_m$  is the mean energy  $E_m = \Sigma E_i \cdot \Phi_i / \Sigma \Phi_i$ ,  $\Phi_i$  being the fluence in the i-th energy bin.

- EH21 is the energy of a monoenergetic field with integral fluence F and integral dose equivalent H21. EH39 and EH60G are similar.

-  $E_{m21}$  is the mean energy  $E_{m21} = \Sigma E_i \cdot H21_i / \Sigma H21_i$ ,  $H21_i$  being the dose equivalent according to ICRP21 in the i-th energy bin.  $E_{m39}$  and  $E_{m60G}$  are similar.

**Explanations to the lower part of a figure:**

- The points represent the ratios *measured/calculated* BS readings,  $r_d$ , obtained according to the Eqs. 1 and 2.

- The left uncertainty bar of a point, in many cases smaller than the point size, indicates the relative statistical uncertainty of the measured reading. The right uncertainty bar includes the relative uncertainty of the calculated reading, which is the  $\sigma_{\text{uncorr}}$  of the fluence response.

- The *reduced chi-squared*,  $X_r^2$ , given in the upper part of the figure is obtained according to the Eq. 7.

**Explanations to the table:**

-  $EL_i$  and  $EU_i$  are the lower and upper margins of the i-th energy bin, respectively;  $E_i = (EL_i \cdot EU_i)^{\frac{1}{2}}$ . All energies are given in eV.

- The solutions are given as spectral fluence  $\Phi_E(E_i) = d\Phi_i/dE_i$  ( $\text{cm}^{-2}\text{eV}^{-1}$ )

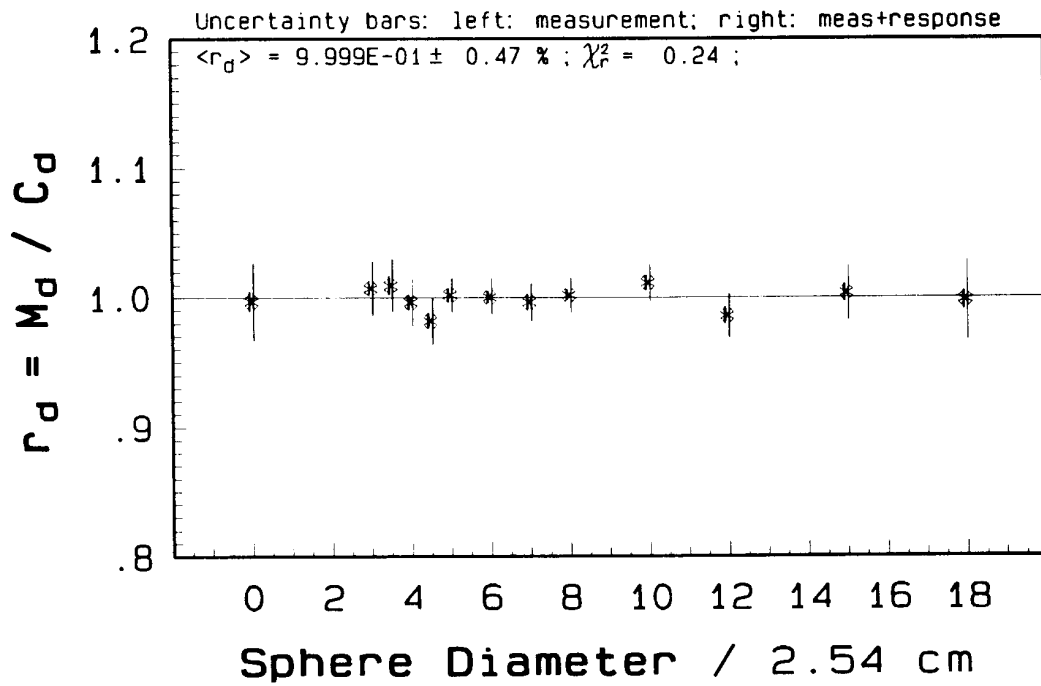
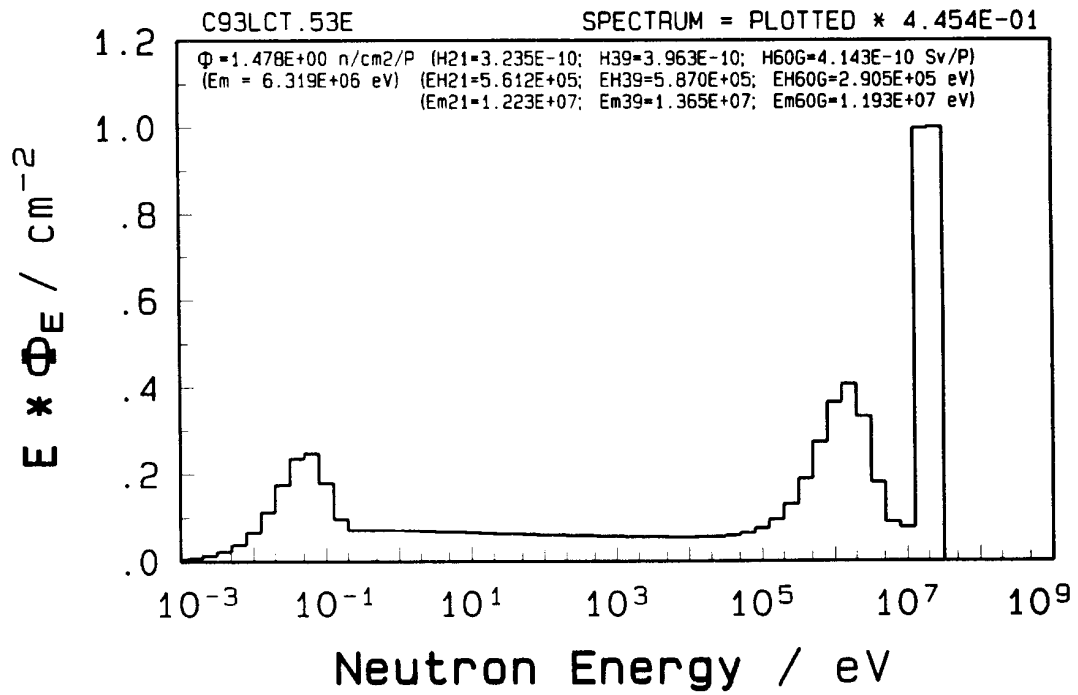


Fig. 8 The PTB-BS solution "53E" for the position CT#6.

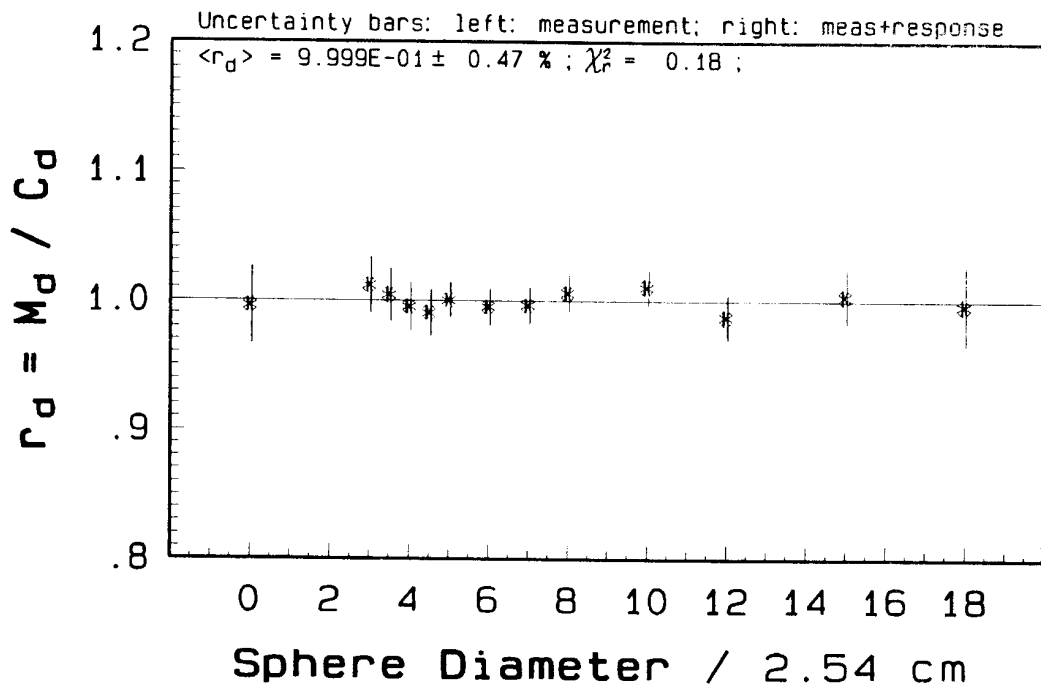
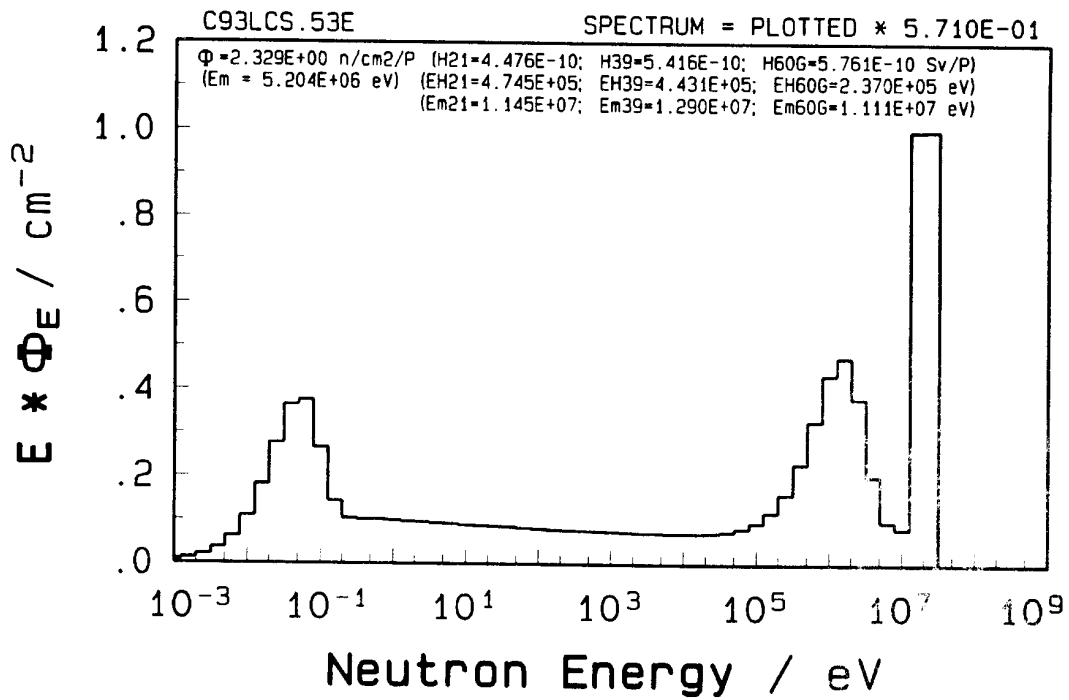


Fig. 9 The PTB-BS solution "53E" for the position CS#2.

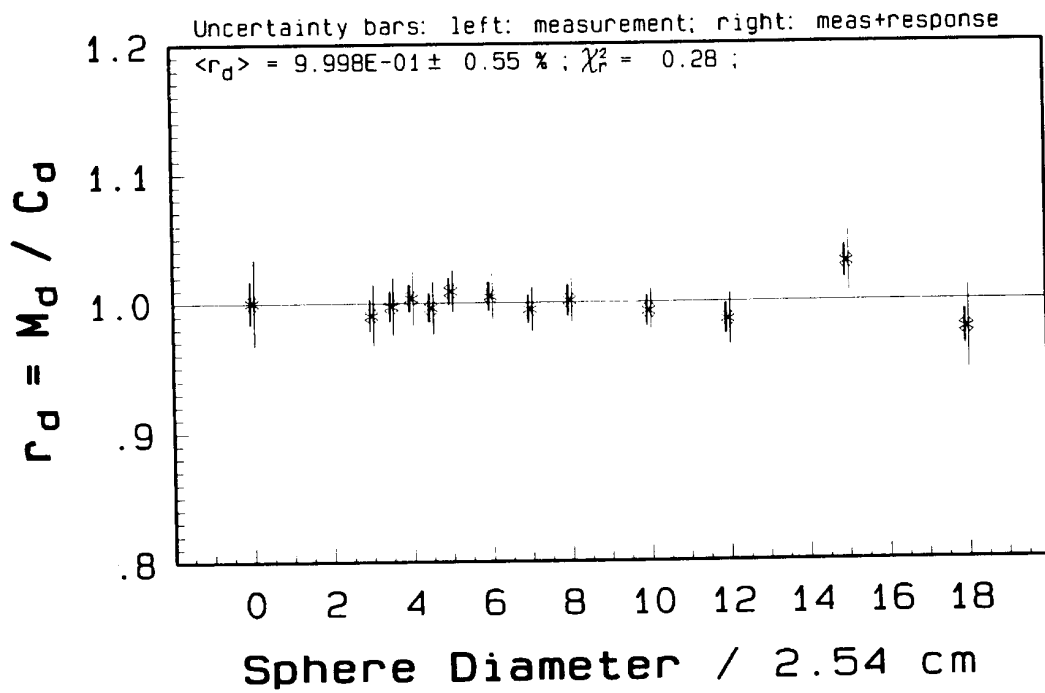
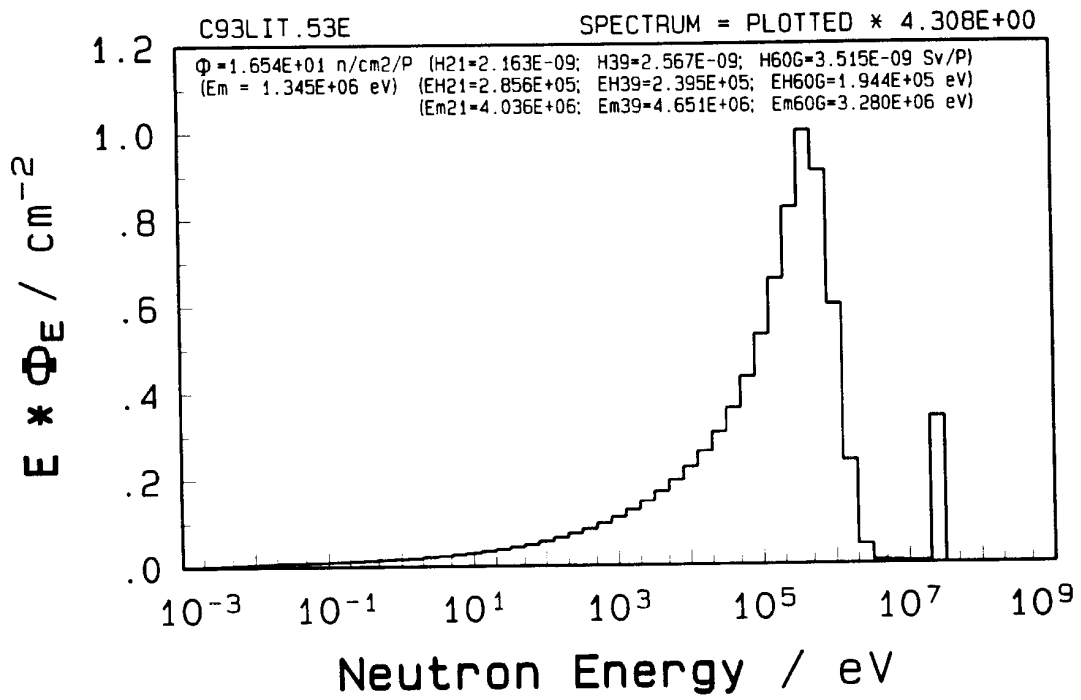


Fig. 10 The PTB-BS solution "53E" for the position IT#6.

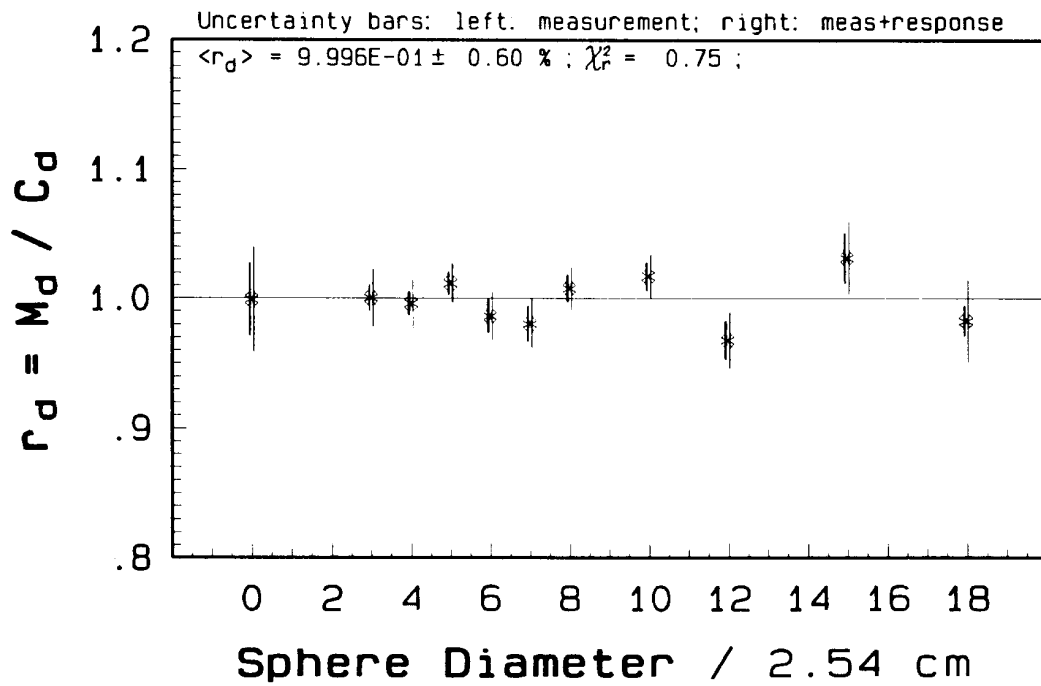
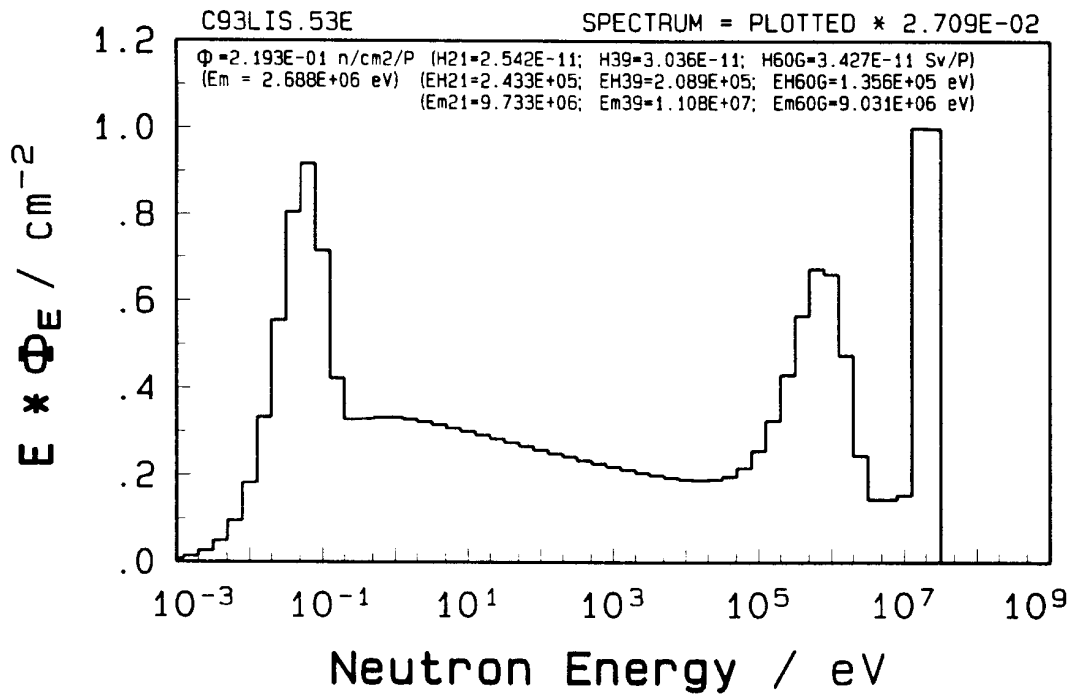


Fig. 11 The PTB-BS solution "53E" for the position IS#4.



Table 6. The PTB-BS solutions "53E" for all four positions.

File C93L4S.53E ( ALEVRA - PTB 7.22 \* 11.02.94 / 12:00:00 )

2  
3 Unfolding BS-measurements! ( code = SANDA5 ; response = C-D\_90.RES )  
4 Data from C93-???.DAT ( CERN - JULY '93 : 4 MEASUREMENT POSITIONS )  
5 13 (11) detectors used: 0C0,3C0,(3C5,)4C0,(4C5,)5C0,6C0,7C0,8C0,10C,12C,15C,18C.  
6 (CT#6) (CS#2) (IT#6) (IS#4)  
7 (Fluence/PIC-count) C93LCT.53E C93LCS.53E C93LIT.53E C93LIS.53E  
8 nE I - Ei(eV) ELi Eui  $\#Ei/cm^2/eV$   $\#Ei/cm^2/eV$   $\#Ei/cm^2/eV$   $\#Ei/cm^2/eV$

53

1	1.0000E-03	7.9433E-04	1.2589E-03	1.8090E+00	4.1240E+00	2.3880E+00	1.8330E-01	
2	1.5849E-03	1.2589E-03	1.9953E-03	1.9680E+00	4.4320E+00	2.4370E+00	2.2510E-01	
3	2.5119E-03	1.9953E-03	3.1623E-03	2.1590E+00	4.7990E+00	2.4640E+00	2.7550E-01	
4	3.9811E-03	3.1623E-03	5.0119E-03	2.3930E+00	5.2380E+00	2.4470E+00	3.3700E-01	
5	6.3096E-03	5.0119E-03	7.9433E-03	2.6670E+00	5.7440E+00	2.3590E+00	4.1080E-01	
6	1.0000E-02	7.9433E-03	1.2589E-02	2.9520E+00	6.2440E+00	2.1650E+00	4.9320E-01	
7	1.5849E-02	1.2589E-02	1.9953E-02	3.1550E+00	6.5470E+00	1.8310E+00	5.6780E-01	
8	2.5119E-02	1.9953E-02	3.1623E-02	3.0920E+00	6.2900E+00	1.3590E+00	5.9830E-01	
9	3.9811E-02	3.1623E-02	5.0119E-02	2.6290E+00	5.2380E+00	9.2200E-01	5.4810E-01	
10	6.3096E-02	5.0119E-02	7.9433E-02	1.7450E+00	3.4070E+00	6.2840E-01	3.9340E-01	
11	1.0000E-01	7.9433E-02	1.2589E-01	7.9360E-01	1.5200E+00	4.3010E-01	1.9370E-01	
12	1.5849E-01	1.2589E-01	1.9953E-01	2.7320E-01	5.1430E-01	2.9550E-01	7.2140E-02	
13	2.5119E-01	1.9953E-01	3.1623E-01	1.2740E-01	2.3640E-01	2.0390E-01	3.5310E-02	
14	3.9811E-01	3.1623E-01	5.0119E-01	7.9260E-02	1.4530E-01	1.4130E-01	2.2370E-02	
15	6.3096E-01	5.0119E-01	7.9433E-01	5.0150E-02	9.0980E-02	9.8430E-02	1.4290E-02	
16	1.0000E+00	7.9433E-01	1.2589E+00	3.1470E-02	5.6570E-02	6.8950E-02	9.0080E-03	
17	1.5849E+00	1.2589E+00	1.9953E+00	1.9610E-02	3.4960E-02	4.8600E-02	5.6160E-03	
18	2.5119E+00	1.9953E+00	3.1623E+00	1.2190E-02	2.1570E-02	3.4420E-02	3.4760E-03	
19	3.9811E+00	3.1623E+00	5.0119E+00	7.5690E-03	1.3310E-02	2.4480E-02	2.1460E-03	
20	6.3096E+00	5.0119E+00	7.9433E+00	4.6970E-03	8.2080E-03	1.7470E-02	1.3210E-03	
21	1.0000E+01	7.9433E+00	1.2589E+01	2.9150E-03	5.0660E-03	1.2500E-02	8.1110E-04	
22	1.5849E+01	1.2589E+01	1.9953E+01	1.8090E-03	3.1290E-03	8.9700E-03	4.9740E-04	
23	2.5119E+01	1.9953E+01	3.1623E+01	1.1240E-03	1.9340E-03	6.4480E-03	3.0470E-04	
24	3.9811E+01	3.1623E+01	5.0119E+01	6.9840E-04	1.1970E-03	4.6420E-03	1.8650E-04	
25	6.3096E+01	5.0119E+01	7.9433E+01	4.3440E-04	7.4110E-04	3.3460E-03	1.1410E-04	
26	1.0000E+02	7.9433E+01	1.2589E+02	2.7020E-04	4.5910E-04	2.4150E-03	6.9790E-05	
27	1.5849E+02	1.2589E+02	1.9953E+02	1.6820E-04	2.8460E-04	1.7440E-03	4.2650E-05	
28	2.5119E+02	1.9953E+02	3.1623E+02	1.0470E-04	1.7640E-04	1.2620E-03	2.6050E-05	
29	3.9811E+02	3.1623E+02	5.0119E+02	6.5180E-05	1.0940E-04	9.1330E-04	1.5910E-05	
30	6.3096E+02	5.0119E+02	7.9433E+02	4.0630E-05	6.7940E-05	6.6140E-04	9.7220E-06	
31	1.0000E+03	7.9433E+02	1.2589E+03	2.5340E-05	4.2220E-05	4.7920E-04	5.9400E-06	
32	1.5849E+03	1.2589E+03	1.9953E+03	1.5820E-05	2.6260E-05	3.4730E-04	3.6300E-06	
33	2.5119E+03	1.9953E+03	3.1623E+03	9.8860E-06	1.6350E-05	2.5190E-04	2.2200E-06	
34	3.9811E+03	3.1623E+03	5.0119E+03	6.1890E-06	1.0200E-05	1.8290E-04	1.3590E-06	
35	6.3096E+03	5.0119E+03	7.9433E+03	3.8840E-06	6.3780E-06	1.3300E-04	8.3480E-07	
36	1.0000E+04	7.9433E+03	1.2589E+04	2.4470E-06	4.0040E-06	9.6920E-05	5.1520E-07	
37	1.5849E+04	1.2589E+04	1.9953E+04	1.5540E-06	2.5330E-06	7.0970E-05	3.2120E-07	
38	2.5119E+04	1.9953E+04	3.1623E+04	1.0010E-06	1.6240E-06	5.2330E-05	2.0410E-07	
39	3.9811E+04	3.1623E+04	5.0119E+04	6.6070E-07	1.0680E-06	3.9020E-05	1.3410E-07	
40	6.3096E+04	5.0119E+04	7.9433E+04	4.5540E-07	7.3240E-07	2.9560E-05	9.2950E-08	
41	1.0000E+05	7.9433E+04	1.2589E+05	3.3490E-07	5.3550E-07	2.2810E-05	6.9260E-08	
42	1.5849E+05	1.2589E+05	1.9953E+05	2.6740E-07	4.2460E-07	1.7900E-05	5.5500E-08	
43	2.5119E+05	1.9953E+05	3.1623E+05	2.3140E-07	3.6450E-07	1.4100E-05	4.6530E-08	
44	3.9811E+05	3.1623E+05	5.0119E+05	2.1110E-07	3.2950E-07	1.0820E-05	3.8580E-08	
45	6.3096E+05	5.0119E+05	7.9433E+05	1.9240E-07	2.9710E-07	6.1880E-06	2.8930E-08	
46	1.0000E+06	7.9433E+05	1.2589E+06	1.6260E-07	2.4780E-07	2.5820E-06	1.7900E-08	
47	1.5849E+06	1.2589E+06	1.9953E+06	1.1430E-07	1.7120E-07	6.4510E-07	8.1400E-09	
48	2.5119E+06	1.9953E+06	3.1623E+06	5.8820E-08	8.6390E-08	7.5110E-08	2.6360E-09	
49	3.9811E+06	3.1623E+06	5.0119E+06	2.0120E-08	2.8890E-08	7.2170E-09	9.8710E-10	
50	6.3096E+06	5.0119E+06	7.9433E+06	6.3000E-09	8.7840E-09	3.0660E-09	6.1970E-10	
51	1.0000E+07	7.9433E+06	1.2589E+07	3.4030E-09	4.6270E-09	1.7380E-09	4.1780E-10	
52	1.5849E+07	1.2589E+07	1.9953E+07	2.8020E-08	3.5950E-08	9.7710E-10	1.7090E-09	
53	2.5119E+07	1.9953E+07	3.1623E+07	1.7730E-08	2.2730E-08	5.7910E-08	1.0760E-09	
$\#total (n/cm^2PIC-count)$				=	1.4775E+00	2.3286E+00	1.6538E+01	2.1929E-01

## APPENDIX C

THE PTB-BS SOLUTIONS (TYPE "61E") FOR ALL FOUR MEASUREMENT  
POSITIONS USING THE FLUENCE RESPONSE MATRIX C-1\_94.A61.

All the data are given per PIC count !

In constructing the *input spectra* the same parameters as for the "53E" solutions were used for neutron energies below 12.59 MeV. For energies beyond this limit a Maxwellian spectral distribution with the maximum at about 80 MeV was introduced to account for a *spallation* reaction assumed to be the main contributor at high energies.

**Explanations to the upper part of a figure:**

- The solution spectrum is plotted as a histogram. In order to get the spectrum in absolute values per PIC count, the plotted values must be multiplied by the factor given in the upper right part of the figure.
- $F$  is the integral fluence in  $\text{cm}^{-2}$ .
- H21, H39 and H60G are the integral dose equivalent according to ICRP21, ICRU39 and ICRP60, respectively, in Sv (see Section 5.3).
- $E_m$  is the mean energy  $E_m = \sum E_i \cdot \phi_i / \sum \phi_i$ ,  $\phi_i$  being the fluence in the  $i$ -th energy bin.
- EH21 is the energy of a monoenergetic field with integral fluence  $F$  and integral dose equivalent H21. EH39 and EH60G are similar.
- $E_{m,21}$  is the mean energy  $E_{m,21} = \sum E_i \cdot H21_i / \sum H21_i$ ,  $H21_i$  being the dose equivalent according to ICRP21 in the  $i$ -th energy bin.  $E_{m,39}$  and  $E_{m,60G}$  are similar.

**Explanations to the lower part of a figure:**

- The points represent the ratios *measured/calculated* BS readings,  $r_d$ , obtained according to the Eqs. 1 and 2.
- The left uncertainty bar of a point, in many cases smaller than the point size, indicates the relative statistical uncertainty of the measured reading. The right uncertainty bar includes the relative uncertainty of the calculated reading, which is the  $\sigma_{\text{uncorr}}$  of the fluence response.
- The *reduced chi-squared*,  $X_r^2$ , given in the upper part of the figure is obtained according to the Eq. 7.

**Explanations to the table:**

- $EL_i$  and  $EU_i$  are the lower and upper margins of the  $i$ -th energy bin, respectively;  $E_i = (EL_i \cdot EU_i)^{\frac{1}{2}}$ . All energies are given in eV.
- The solutions are given as spectral fluence  $\phi_E(E_i) = d\phi_i / dE_i$  ( $\text{cm}^{-2} \text{eV}^{-1}$ )

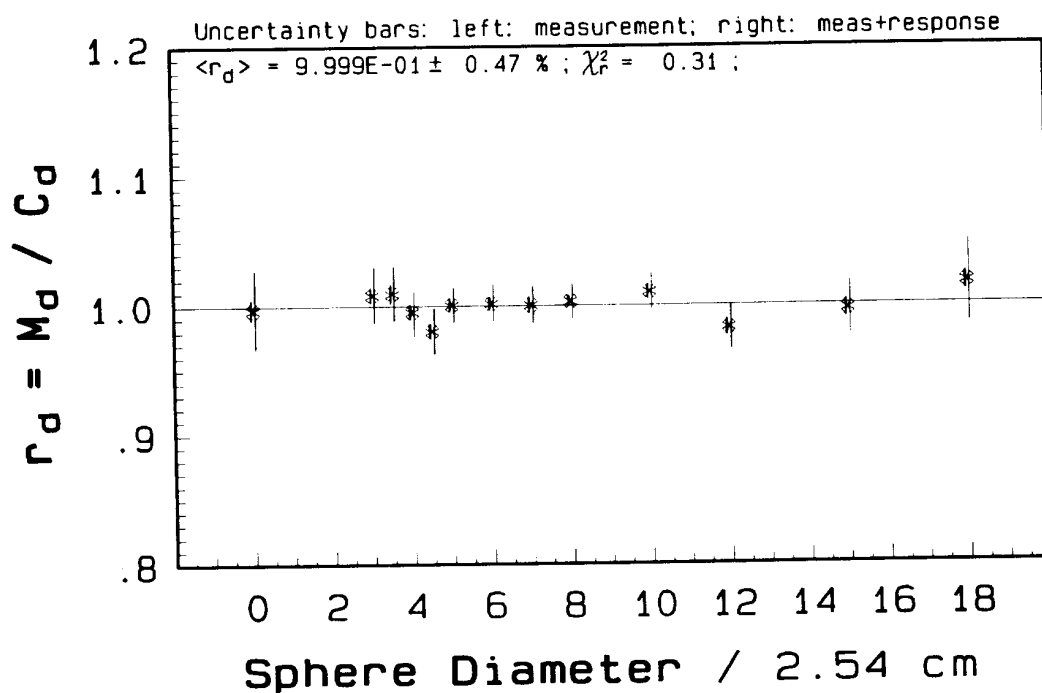
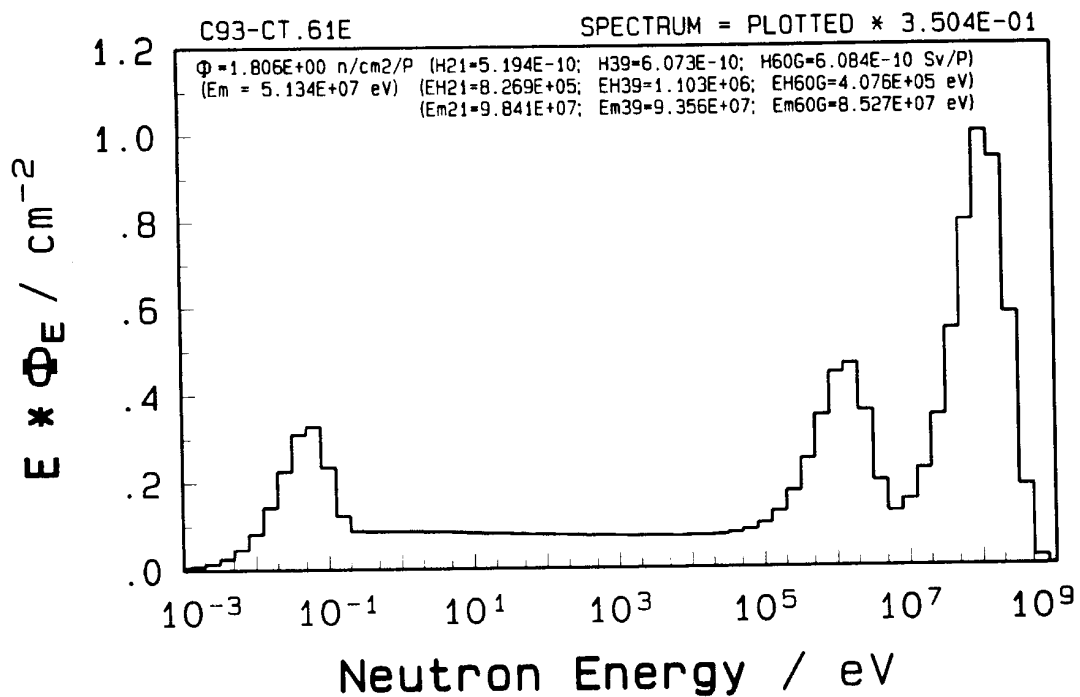


Fig. 12 The PTB-BS solution "61E" for the position CT#6.

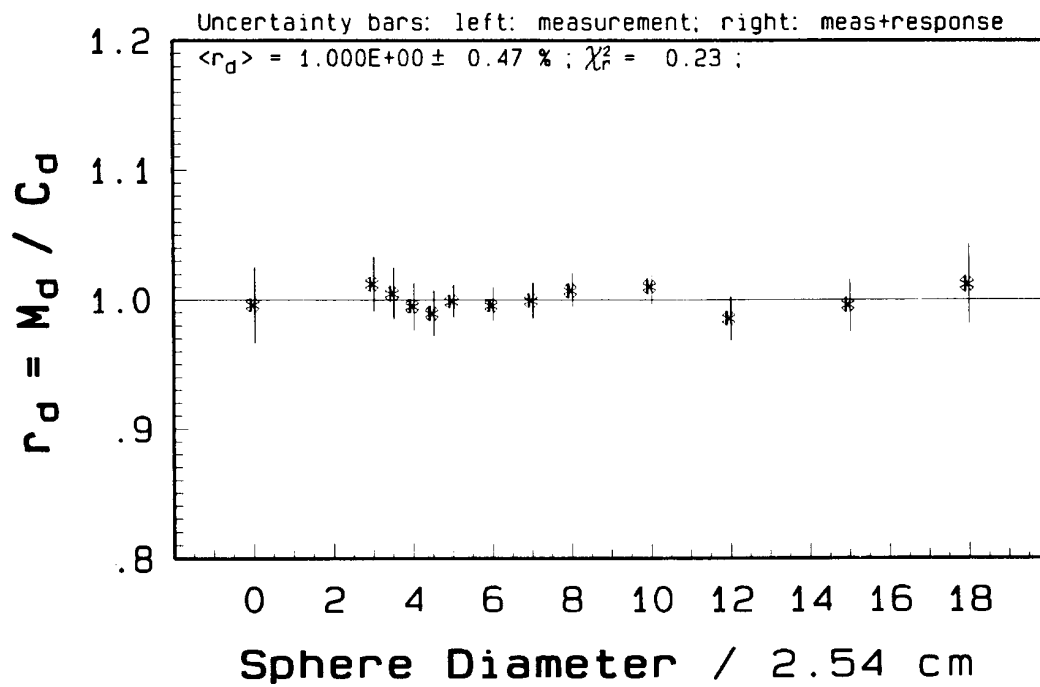
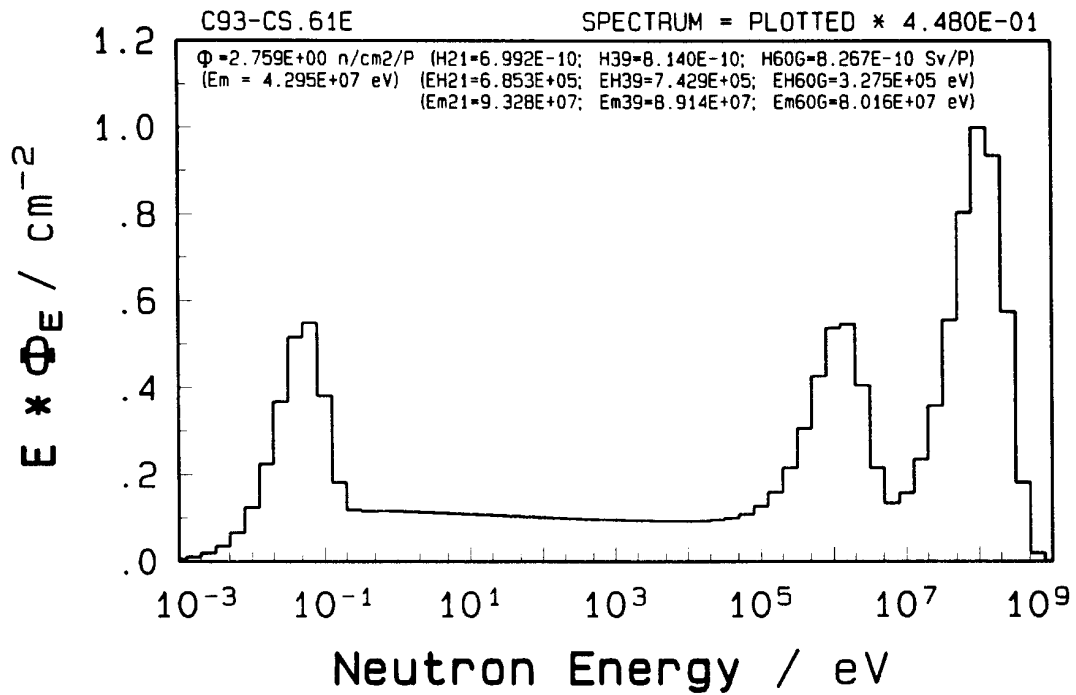


Fig. 13 The PTB-BS solution "61E" for the position CS#2.

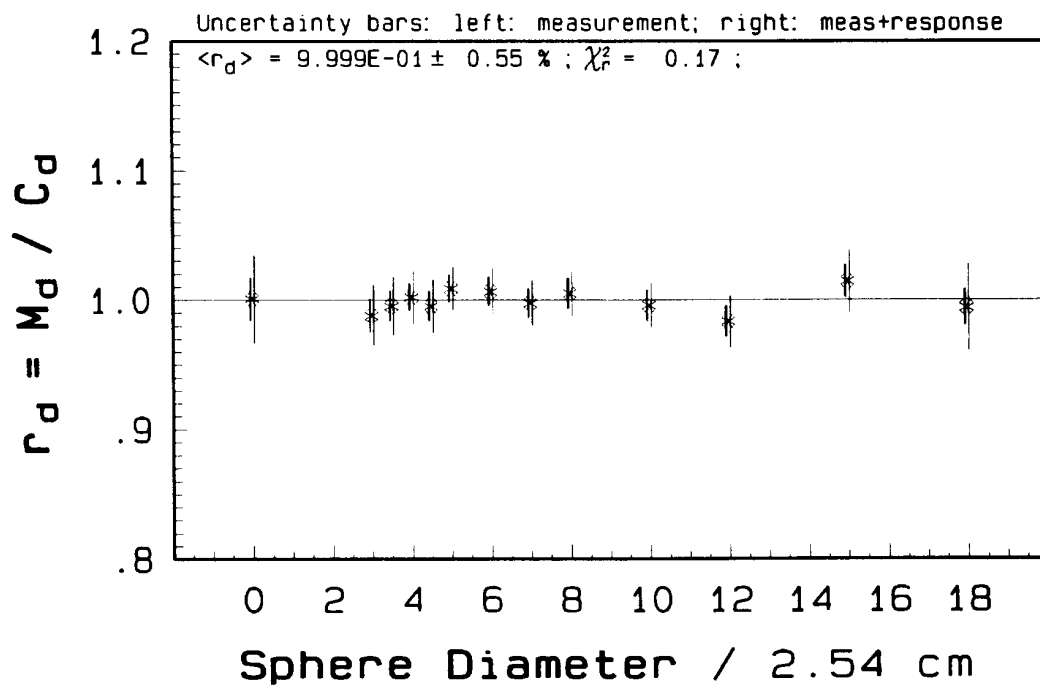
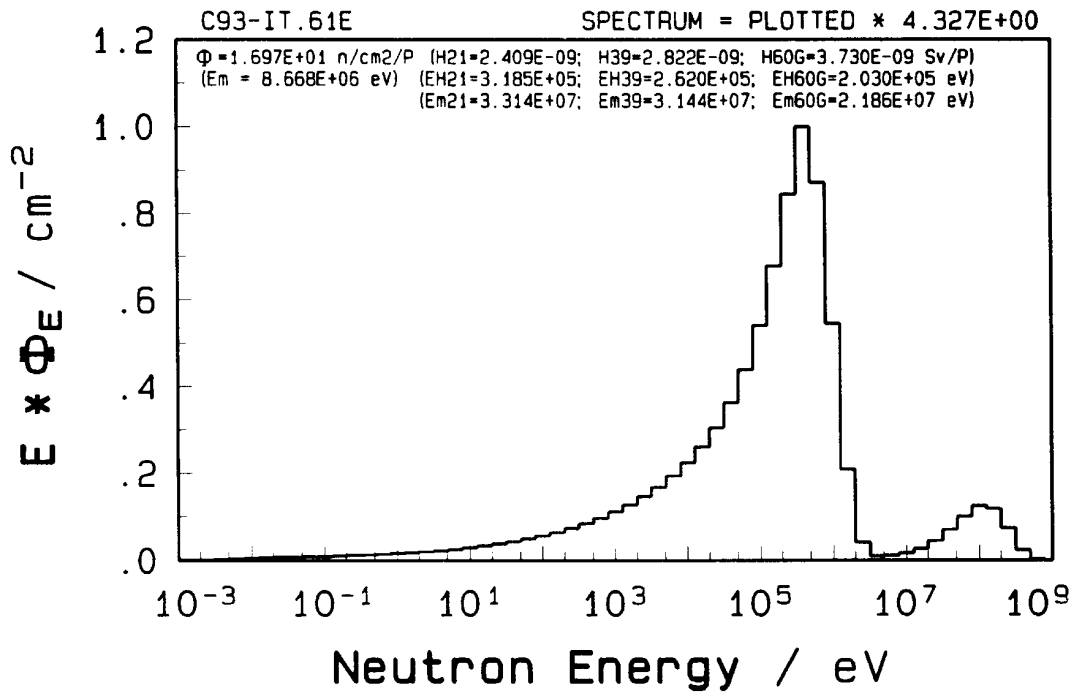


Fig. 14 The PTB-BS solution "61E" for the position IT#6.

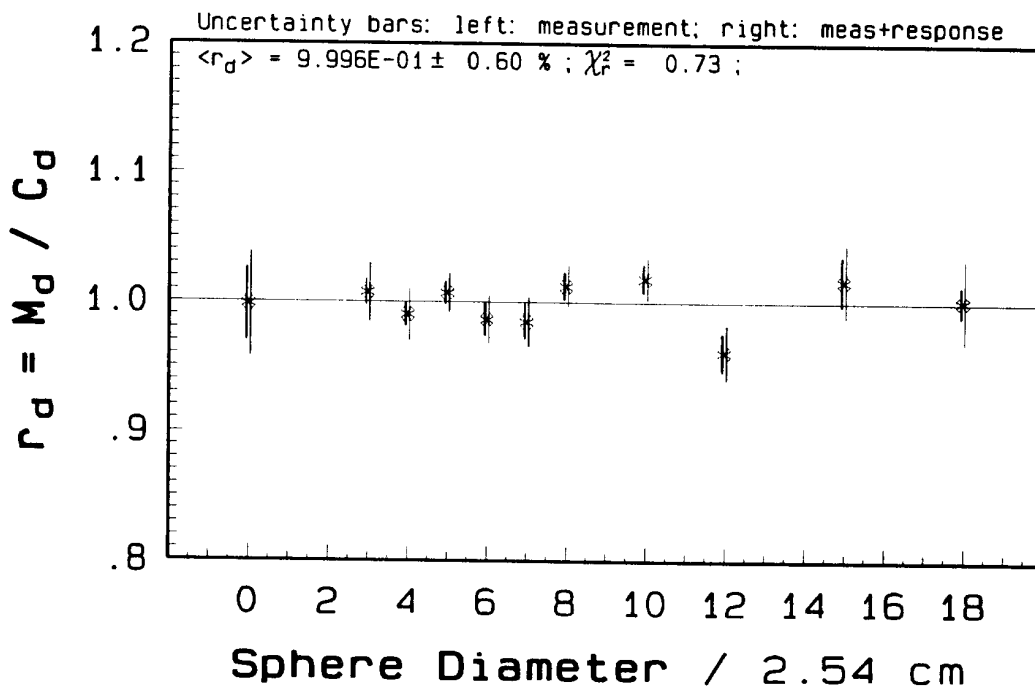
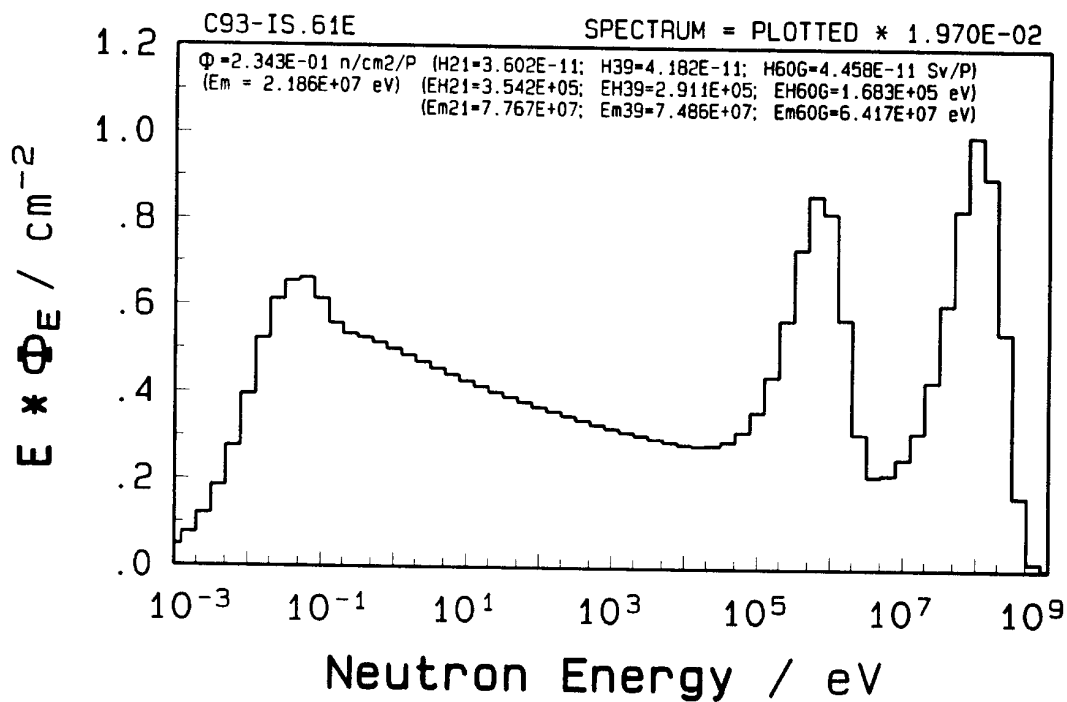


Fig. 15 The PTB-BS solution "61E" for the position IS#4.

Table 7. The PTB-BS solutions "61E" for all four positions.

File C93-4S.61E ( ALEVRA - PTB 7.22 \* 11.02.94 / 12:00:00 )

Unfolding BS-measurements! ( code = SANDA7 ; response = C-1.94.A61 )							
Data from C93-???.DAT ( CERN - JULY '93 : 4 MEASUREMENT POSITIONS )							
13 (11) detectors used: 0C0,3C0,(3C5,)4C0,(4C5,)5C0,6C0,7C0,8C0,10C,12C,15C,18C.							
		(CT#6)		(CS#2)		(IT#6)	
(Fluence/PIC-count)		C93-CT.61E		C93-CS.61E		C93-IT.61E	
nE	I = Ei(eV)	ELi	EUi	⊕Ei/cm²/eV	⊕Ei/cm²/eV	⊕Ei/cm²/eV	⊕Ei/cm²/eV
61							
1	1.0000E-03	7.9433E-04	1.2589E-03	1.5850E+00	2.5420E+00	2.4810E+00	9.4820E-01
2	1.5849E-03	1.2589E-03	1.9953E-03	1.7490E+00	2.8930E+00	2.5200E+00	9.5190E-01
3	2.5119E-03	1.9953E-03	3.1623E-03	1.9520E+00	3.3430E+00	2.5340E+00	9.4360E-01
4	3.9811E-03	3.1623E-03	5.0119E-03	2.2070E+00	3.9280E+00	2.5040E+00	9.1780E-01
5	6.3096E-03	5.0119E-03	7.9433E-03	2.5170E+00	4.6720E+00	2.4010E+00	8.6640E-01
6	1.0000E-02	7.9433E-03	1.2589E-02	2.8570E+00	5.5330E+00	2.1900E+00	7.7960E-01
7	1.5849E-02	1.2589E-02	1.9953E-02	3.1320E+00	6.3120E+00	1.8430E+00	6.5030E-01
8	2.5119E-02	1.9953E-02	3.1623E-02	3.1450E+00	6.5600E+00	1.3610E+00	4.8140E-01
9	3.9811E-02	3.1623E-02	5.0119E-02	2.7220E+00	5.8070E+00	9.1920E-01	3.2470E-01
10	6.3096E-02	5.0119E-02	7.9433E-02	1.8210E+00	3.8980E+00	6.2390E-01	2.0690E-01
11	1.0000E-01	7.9433E-02	1.2589E-01	8.1930E-01	1.7100E+00	4.2570E-01	1.2100E-01
12	1.5849E-01	1.2589E-01	1.9953E-01	2.6940E-01	5.1370E-01	2.9190E-01	6.9320E-02
13	2.5119E-01	1.9953E-01	3.1623E-01	1.2090E-01	2.1060E-01	2.0120E-01	4.1940E-02
14	3.9811E-01	3.1623E-01	5.0119E-01	7.5210E-02	1.2970E-01	1.3940E-01	2.5990E-02
15	6.3096E-01	5.0119E-01	7.9433E-01	4.7800E-02	8.2280E-02	9.7120E-02	1.6050E-02
16	1.0000E+00	7.9433E-01	1.2589E+00	3.0130E-02	5.1740E-02	6.8080E-02	9.8680E-03
17	1.5849E+00	1.2589E+00	1.9953E+00	1.8860E-02	3.2310E-02	4.8040E-02	6.0410E-03
18	2.5119E+00	1.9953E+00	3.1623E+00	1.1770E-02	2.0110E-02	3.4060E-02	3.6940E-03
19	3.9811E+00	3.1623E+00	5.0119E+00	7.3460E-03	1.2510E-02	2.4250E-02	2.2590E-03
20	6.3096E+00	5.0119E+00	7.9433E+00	4.5780E-03	7.7770E-03	1.7330E-02	1.3810E-03
21	1.0000E+01	7.9433E+00	1.2589E+01	2.8530E-03	4.8340E-03	1.2410E-02	8.4480E-04
22	1.5849E+01	1.2589E+01	1.9953E+01	1.7780E-03	3.0050E-03	8.9140E-03	5.1690E-04
23	2.5119E+01	1.9953E+01	3.1623E+01	1.1090E-03	1.8690E-03	6.4120E-03	3.1630E-04
24	3.9811E+01	3.1623E+01	5.0119E+01	6.9190E-04	1.1640E-03	4.6180E-03	1.9370E-04
25	6.3096E+01	5.0119E+01	7.9433E+01	4.3200E-04	7.2460E-04	3.3300E-03	1.1870E-04
26	1.0000E+02	7.9433E+01	1.2589E+02	2.6970E-04	4.5140E-04	2.4040E-03	7.2750E-05
27	1.5849E+02	1.2589E+02	1.9953E+02	1.6850E-04	2.8130E-04	1.7370E-03	4.4600E-05
28	2.5119E+02	1.9953E+02	3.1623E+02	1.0530E-04	1.7530E-04	1.2570E-03	2.7350E-05
29	3.9811E+02	3.1623E+02	5.0119E+02	6.5800E-05	1.0930E-04	9.0990E-04	1.6780E-05
30	6.3096E+02	5.0119E+02	7.9433E+02	4.1160E-05	6.8230E-05	6.5900E-04	1.0300E-05
31	1.0000E+03	7.9433E+02	1.2589E+03	2.5770E-05	4.2610E-05	4.7750E-04	6.3280E-06
32	1.5849E+03	1.2589E+03	1.9953E+03	1.6140E-05	2.6630E-05	3.4610E-04	3.8900E-06
33	2.5119E+03	1.9953E+03	3.1623E+03	1.0120E-05	1.6660E-05	2.5100E-04	2.3930E-06
34	3.9811E+03	3.1623E+03	5.0119E+03	6.3580E-06	1.0440E-05	1.8220E-04	1.4740E-06
35	6.3096E+03	5.0119E+03	7.9433E+03	4.0030E-06	6.5590E-06	1.3260E-04	9.1030E-07
36	1.0000E+04	7.9433E+03	1.2589E+04	2.5300E-06	4.1370E-06	9.6720E-05	5.6430E-07
37	1.5849E+04	1.2589E+04	1.9953E+04	1.6110E-06	2.6280E-06	7.0960E-05	3.5250E-07
38	2.5119E+04	1.9953E+04	3.1623E+04	1.0410E-06	1.6930E-06	5.2510E-05	2.2340E-07
39	3.9811E+04	3.1623E+04	5.0119E+04	6.8900E-07	1.1180E-06	3.9370E-05	1.4520E-07
40	6.3096E+04	5.0119E+04	7.9433E+04	4.7590E-07	7.6970E-07	3.0060E-05	9.8530E-08
41	1.0000E+05	7.9433E+04	1.2589E+05	3.5030E-07	5.6460E-07	2.3420E-05	7.1070E-08
42	1.5849E+05	1.2589E+05	1.9953E+05	2.7930E-07	4.4840E-07	1.8530E-05	5.4960E-08
43	2.5119E+05	1.9953E+05	3.1623E+05	2.4060E-07	3.8450E-07	1.4550E-05	4.4800E-08
44	3.9811E+05	3.1623E+05	5.0119E+05	2.1680E-07	3.4420E-07	1.0870E-05	3.6450E-08
45	6.3096E+05	5.0119E+05	7.9433E+05	1.9260E-07	3.0270E-07	5.9730E-06	2.6840E-08
46	1.0000E+06	7.9433E+05	1.2589E+06	1.5550E-07	2.4060E-07	2.3590E-06	1.6130E-08
47	1.5849E+06	1.2589E+06	1.9953E+06	1.0250E-07	1.5440E-07	5.6710E-07	7.1300E-09
48	2.5119E+06	1.9953E+06	3.1623E+06	4.9740E-08	7.2260E-08	6.9270E-08	2.4460E-09
49	3.9811E+06	3.1623E+06	5.0119E+06	1.7250E-08	2.4190E-08	1.0150E-08	1.0570E-09
50	6.3096E+06	5.0119E+06	7.9433E+06	6.9050E-09	9.4440E-09	7.3300E-09	6.8140E-10
51	1.0000E+07	7.9433E+06	1.2589E+07	5.2950E-09	7.0770E-09	6.9870E-09	5.0090E-10
52	1.5849E+07	1.2589E+07	1.9953E+07	4.9220E-09	6.6320E-09	7.1200E-09	3.9270E-10
53	2.5119E+07	1.9953E+07	3.1623E+07	4.8120E-09	6.3940E-09	7.5600E-09	3.3960E-10
54	3.9811E+07	3.1623E+07	5.0119E+07	4.7770E-09	6.2560E-09	7.5270E-09	3.0160E-10
55	6.3096E+07	5.0119E+07	7.9433E+07	4.4050E-09	5.7100E-09	6.8560E-09	2.5840E-10
56	1.0000E+08	7.9433E+07	1.2589E+08	3.5040E-09	4.4800E-09	5.3420E-09	1.9700E-10
57	1.5849E+08	1.2589E+08	1.9953E+08	2.0770E-09	2.6420E-09	3.1990E-09	1.1240E-10
58	2.5119E+08	1.9953E+08	3.1623E+08	8.0900E-10	1.0250E-09	1.2540E-09	4.2670E-11
59	3.9811E+08	3.1623E+08	5.0119E+08	1.6090E-10	2.0410E-10	2.5000E-10	8.3400E-12
60	6.3096E+08	5.0119E+08	7.9433E+08	1.0940E-11	1.3900E-11	1.7090E-11	5.6220E-13
61	1.0000E+09	7.9433E+08	1.2589E+09	1.3640E-13	1.7320E-13	2.1260E-13	6.9510E-15

⊕total (n/cm²PIC-count) = 1.8059E+00 2.7586E+00 1.6974E+01 2.3433E-01

## APPENDIX D

THE PTB-BS SOLUTIONS (TYPE "6IX") FOR ALL FOUR MEASUREMENT  
POSITIONS USING THE FLUENCE RESPONSE MATRIX C-1\_94.A61.

All the data are given per PIC count !

In constructing the *input spectra* the "53E" solutions from Appendix B were used for neutron energies below 10 keV. For energies beyond this limit the numerical results of the calculations presented in Ref. 3 were used. The calculated spectra were rebinned to match our responses and normalized to one PIC count.

**Explanations to the upper part of a figure:**

- The solution spectrum is plotted as a histogram. In order to get the spectrum in absolute values per PIC count, the plotted values must be multiplied by the factor given in the upper right part of the figure.
- $F$  is the integral fluence in  $\text{cm}^{-2}$ .
- H21, H39 and H60G are the integral dose equivalent according to ICRP21, ICRU39 and ICRP60, respectively, in Sv (see Section 5.3).
- $E_m$  is the mean energy  $E_m = \sum E_i \cdot \Phi_i / \sum \Phi_i$ ,  $\Phi_i$  being the fluence in the  $i$ -th energy bin.
- EH21 is the energy of a monoenergetic field with integral fluence  $F$  and integral dose equivalent H21. EH39 and EH60G are similar.
- $E_{m21}$  is the mean energy  $E_{m21} = \sum E_i \cdot H21_i / \sum H21_i$ ,  $H21_i$  being the dose equivalent according to ICRP21 in the  $i$ -th energy bin.  $E_{m39}$  and  $E_{m60G}$  are similar.

**Explanations to the lower part of a figure:**

- The points represent the ratios *measured/calculated* BS readings,  $r_d$ , obtained according to the Eqs. 1 and 2.
- The left uncertainty bar of a point, in many cases smaller than the point size, indicates the relative statistical uncertainty of the measured reading. The right uncertainty bar includes the relative uncertainty of the calculated reading, which is the  $\sigma_{\text{uncorr}}$  of the fluence response.
- The *reduced chi-squared*,  $\chi_r^2$ , given in the upper part of the figure is obtained according to the Eq. 7.

**Explanations to the table:**

- $EL_i$  and  $EU_i$  are the lower and upper margins of the  $i$ -th energy bin, respectively;  $E_i = (EL_i \cdot EU_i)^{\frac{1}{2}}$ . All energies are given in eV.
- The solutions are given as spectral fluence  $\Phi_E(E_i) = d\Phi_i/dE_i$  ( $\text{cm}^{-2}\text{eV}^{-1}$ )



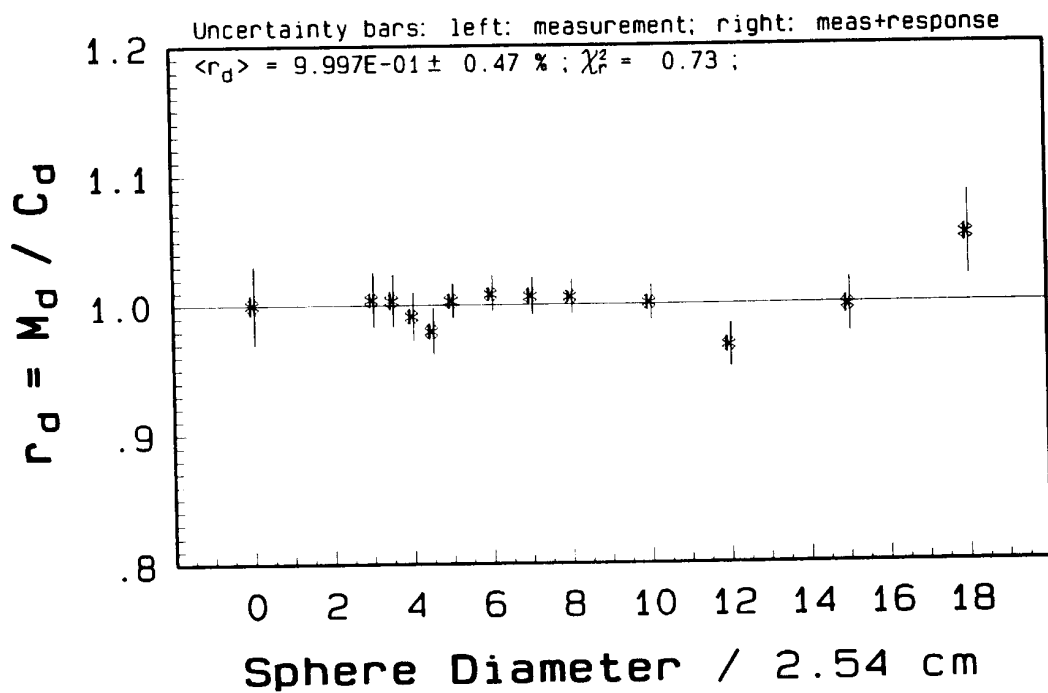
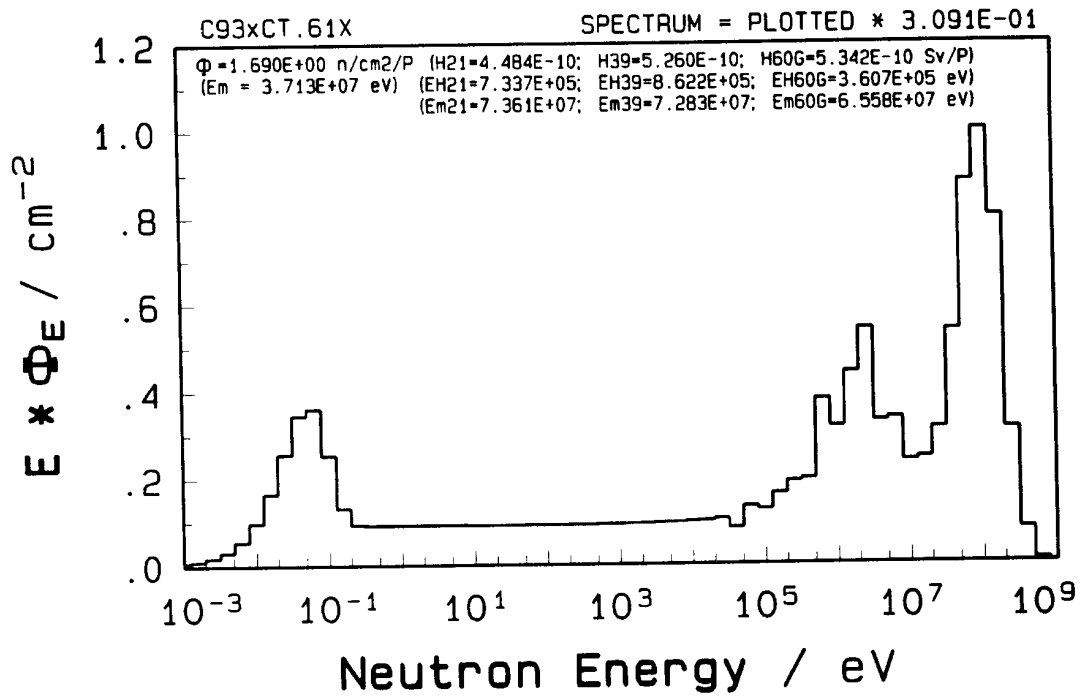


Fig. 16 The PTB-BS solution "61X" for the position CT#6.

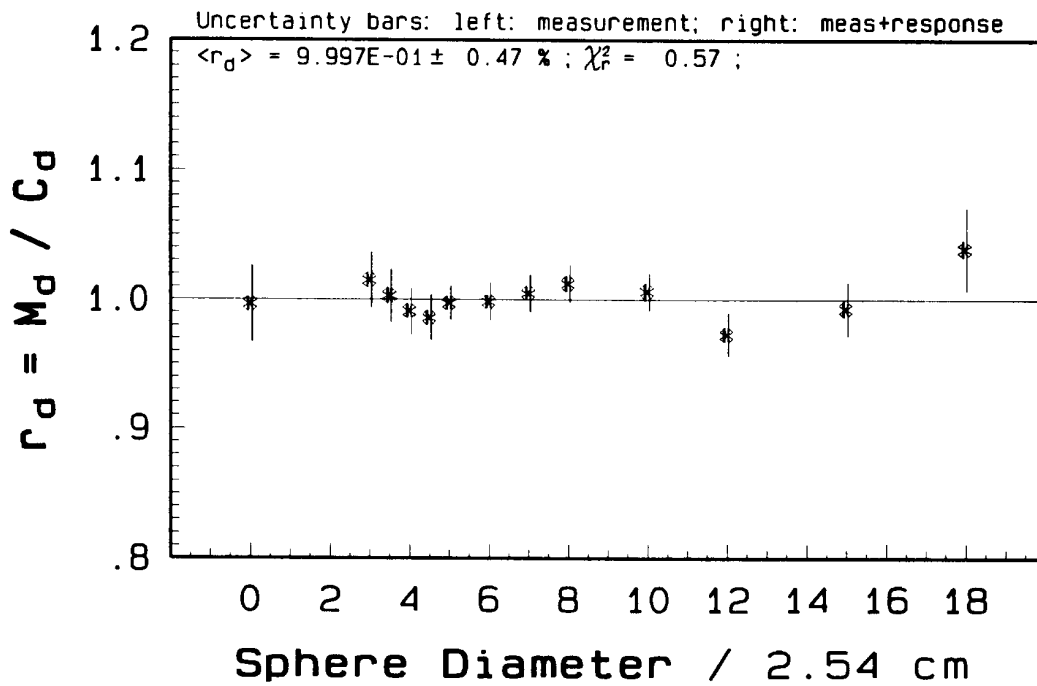
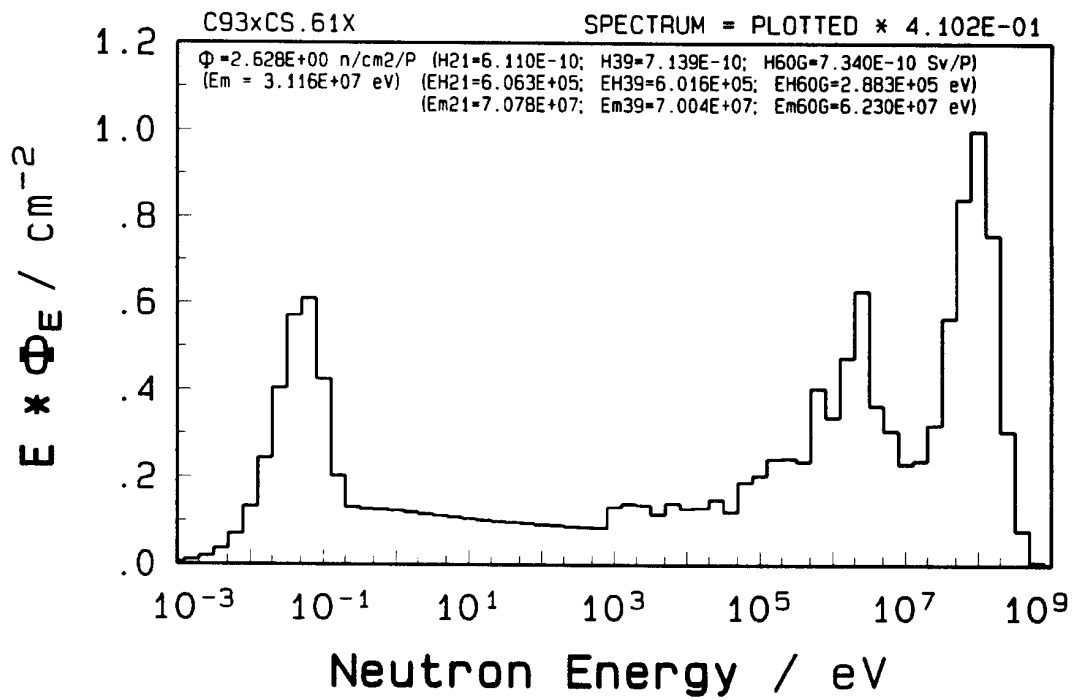


Fig. 17 The PTB-BS solution "6XE" for the position CS#2.

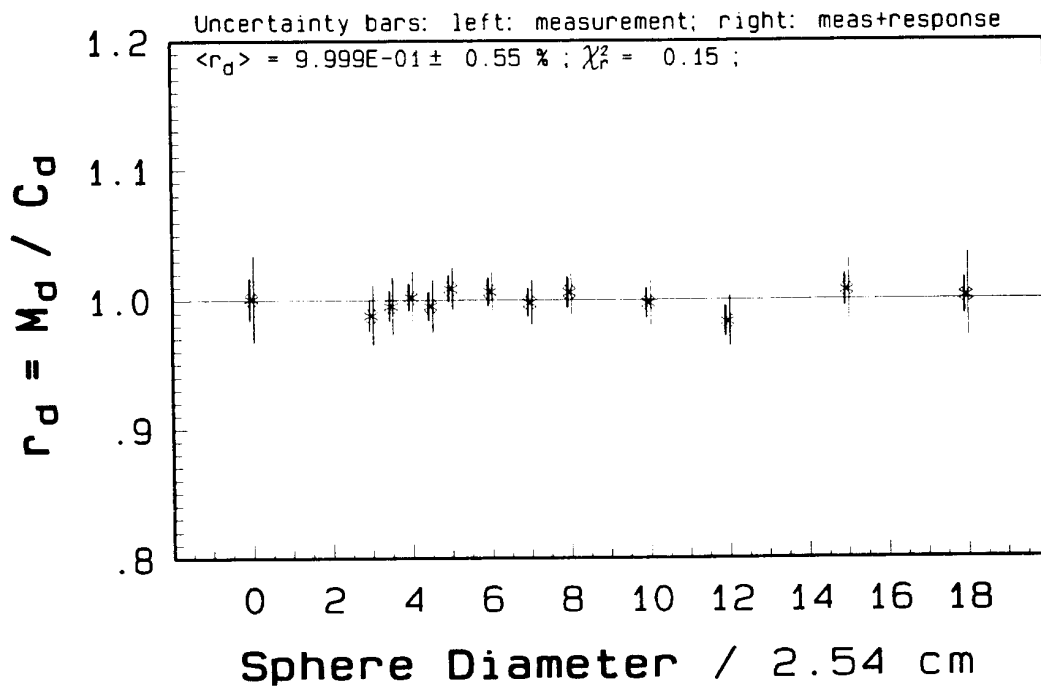
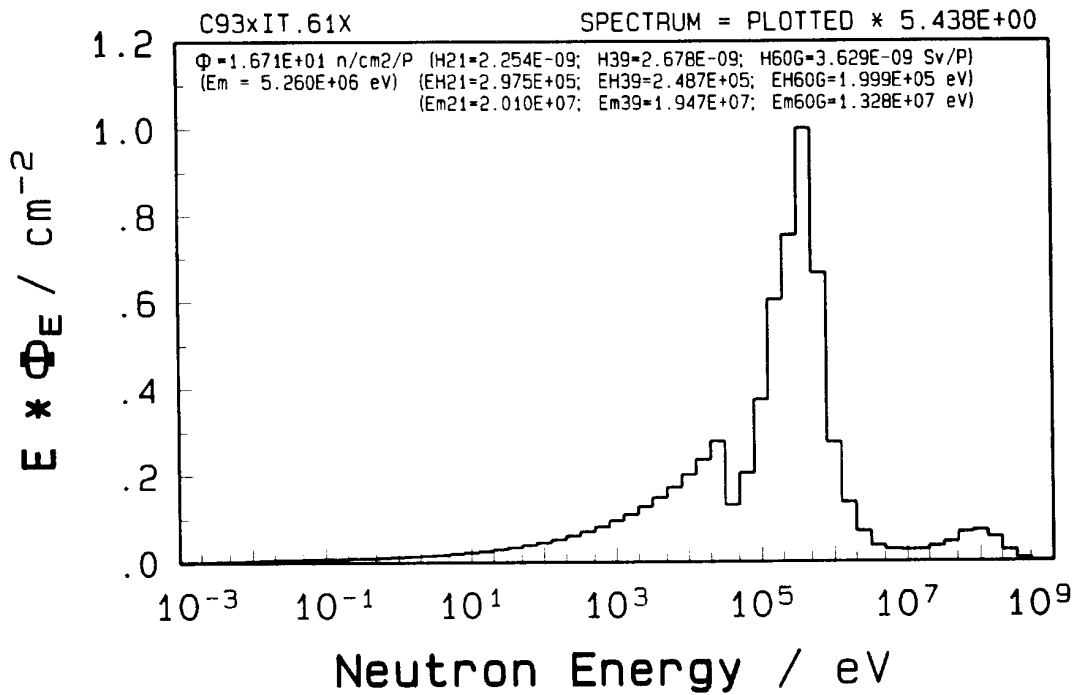


Fig. 18 The PTB-BS solution "61X" for the position IT#6.

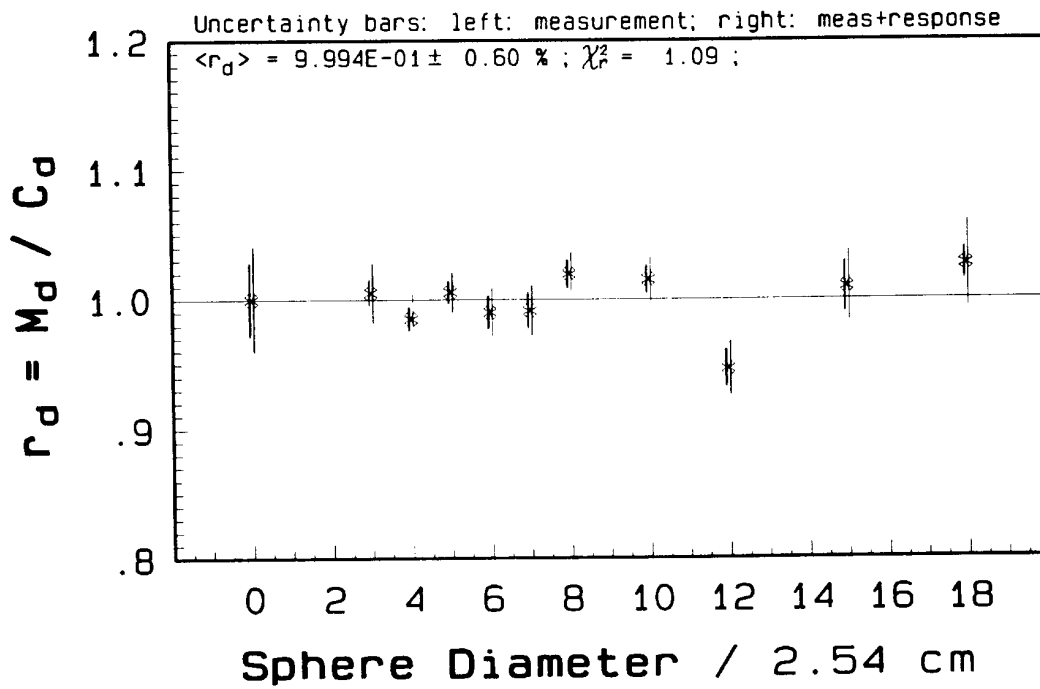
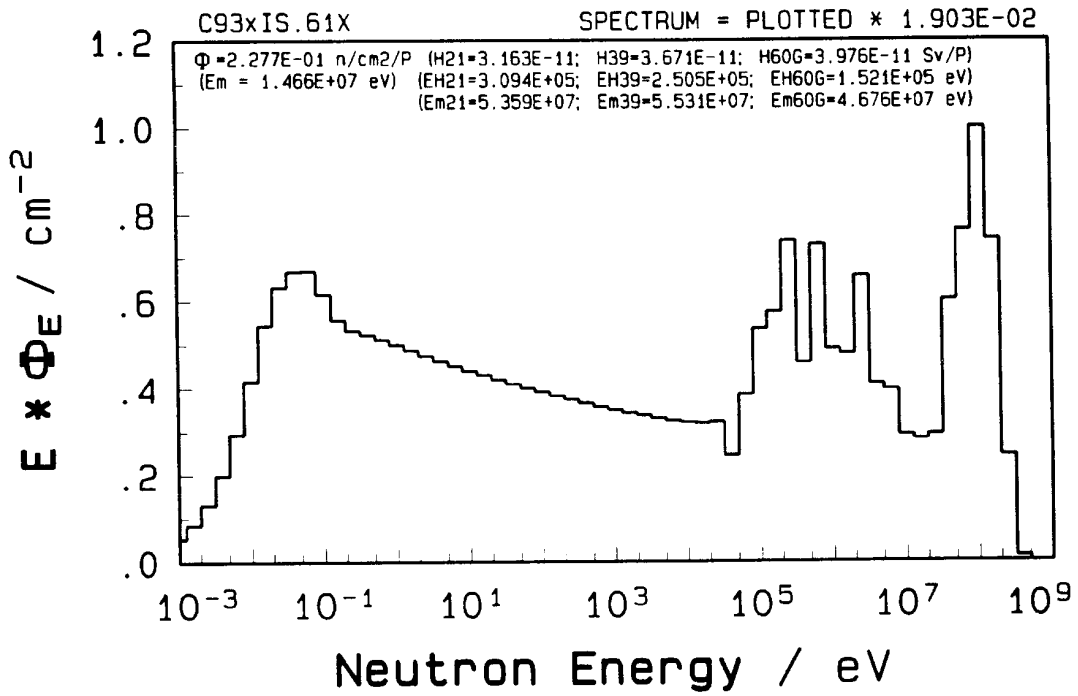


Fig. 19 The PTB-BS solution "61X" for the position IS#4.

Table 8. The PTB-BS solutions "61X" for all four positions.

File C93x4S.61X ( ALEVRA - PTB 7.22 \* 02.03.94 / 18:00:00 )

Unfolding BS-measurements! ( code = SANDA7 ; response = C-1.94.A61 )									
Data from C93-???.DAT ( CERN - JULY '93 : 4 MEASUREMENT POSITIONS )									
13 (11) detectors used: 0C0,3C0,(3C5),4C0,(4C5),5C0,6C0,7C0,8C0,10C,12C,15C,18C.									
[ INPUT = FLUKA + C93L???.53E for En≤10 keV ]		(CT#6)	(CS#2)	(IT#6)	(IS#4)				
(Fluence/PIC-count)	C93xCT.61X	C93xCS.61X	C93xIT.61X	C93xIS.61X					
nE — I — Ei(eV) — ELi — EUi —	‡Ei/cm <sup>2</sup> /eV	‡Ei/cm <sup>2</sup> /eV	‡Ei/cm <sup>2</sup> /eV	‡Ei/cm <sup>2</sup> /eV					
61	1	1.0000E-03	7.9433E-04	1.2589E-03	1.7960E+00	2.2910E+00	2.5760E+00	1.0090E+00	
	2	1.5849E-03	1.2589E-03	1.9953E-03	1.9510E+00	2.6580E+00	2.6120E+00	1.0040E+00	
	3	2.5119E-03	1.9953E-03	3.1623E-03	2.1420E+00	3.1290E+00	2.6220E+00	9.8660E-01	
	4	3.9811E-03	3.1623E-03	5.0119E-03	2.3810E+00	3.7420E+00	2.5860E+00	9.5050E-01	
	5	6.3096E-03	5.0119E-03	7.9433E-03	2.6670E+00	4.5260E+00	2.4730E+00	8.8830E-01	
	6	1.0000E-02	7.9433E-03	1.2589E-02	2.9730E+00	5.4410E+00	2.2490E+00	7.9110E-01	
	7	1.5849E-02	1.2589E-02	1.9953E-02	3.1990E+00	6.2880E+00	1.8850E+00	6.5300E-01	
	8	2.5119E-02	1.9953E-02	3.1623E-02	3.1550E+00	6.6030E+00	1.3850E+00	4.7840E-01	
	9	3.9811E-02	3.1623E-02	5.0119E-02	2.6830E+00	5.8890E+00	9.2980E-01	3.1950E-01	
	10	6.3096E-02	5.0119E-02	7.9433E-02	1.7660E+00	3.9690E+00	6.2610E-01	2.0190E-01	
	11	1.0000E-01	7.9433E-02	1.2589E-01	7.8370E-01	1.7430E+00	4.2300E-01	1.1730E-01	
	12	1.5849E-01	1.2589E-01	1.9953E-01	2.5490E-01	5.2290E-01	2.8660E-01	6.6910E-02	
	13	2.5119E-01	1.9953E-01	3.1623E-01	1.1360E-01	2.1320E-01	1.9500E-01	4.0380E-02	
	14	3.9811E-01	3.1623E-01	5.0119E-01	7.0390E-02	1.3020E-01	1.3330E-01	2.5000E-02	
	15	6.3096E-01	5.0119E-01	7.9433E-01	4.4730E-02	8.1520E-02	9.1880E-02	1.5440E-02	
	16	1.0000E+00	7.9433E-01	1.2589E+00	2.8280E-02	5.0410E-02	6.3950E-02	9.5140E-03	
	17	1.5849E+00	1.2589E+00	1.9953E+00	1.7810E-02	3.0860E-02	4.5060E-02	5.8480E-03	
	18	2.5119E+00	1.9953E+00	3.1623E+00	1.1200E-02	1.8840E-02	3.2050E-02	3.5940E-03	
	19	3.9811E+00	3.1623E+00	5.0119E+00	7.0560E-03	1.1500E-02	2.2930E-02	2.2110E-03	
	20	6.3096E+00	5.0119E+00	7.9433E+00	4.4410E-03	7.0210E-03	1.6520E-02	1.3600E-03	
	21	1.0000E+01	7.9433E+00	1.2589E+01	2.7960E-03	4.2910E-03	1.1940E-02	8.3690E-04	
	22	1.5849E+01	1.2589E+01	1.9953E+01	1.7620E-03	2.6260E-03	8.6660E-03	5.1540E-04	
	23	2.5119E+01	1.9953E+01	3.1623E+01	1.1120E-03	1.6090E-03	6.3050E-03	3.1740E-04	
	24	3.9811E+01	3.1623E+01	5.0119E+01	7.0190E-04	9.8890E-04	4.5950E-03	1.9570E-04	
	25	6.3096E+01	5.0119E+01	7.9433E+01	4.4350E-04	6.0800E-04	3.3530E-03	1.2070E-04	
	26	1.0000E+02	7.9433E+01	1.2589E+02	2.8030E-04	3.7430E-04	2.4500E-03	7.4450E-05	
	27	1.5849E+02	1.2589E+02	1.9953E+02	1.7740E-04	2.3070E-04	1.7910E-03	4.5930E-05	
	28	2.5119E+02	1.9953E+02	3.1623E+02	1.1230E-04	1.4230E-04	1.3120E-03	2.8350E-05	
	29	3.9811E+02	3.1623E+02	5.0119E+02	7.1170E-05	8.7820E-05	9.6070E-04	1.7510E-05	
	30	6.3096E+02	5.0119E+02	7.9433E+02	4.5120E-05	5.4320E-05	7.0360E-04	1.0810E-05	
	31	1.0000E+03	7.9433E+02	1.2589E+03	2.8640E-05	5.3860E-05	5.1530E-04	6.6840E-06	
	32	1.5849E+03	1.2589E+03	1.9953E+03	1.8190E-05	3.5960E-05	3.7720E-04	4.1330E-06	
	33	2.5119E+03	1.9953E+03	3.1623E+03	1.1570E-05	2.2280E-05	2.7610E-04	2.5570E-06	
	34	3.9811E+03	3.1623E+03	5.0119E+03	7.3690E-06	1.1870E-05	2.0220E-04	1.5830E-06	
	35	6.3096E+03	5.0119E+03	7.9433E+03	4.7060E-06	9.1070E-06	1.4830E-04	9.8300E-07	
	36	1.0000E+04	7.9433E+03	1.2589E+04	3.0180E-06	5.2710E-06	1.0900E-04	6.1240E-07	
	37	1.5849E+04	1.2589E+04	1.9953E+04	1.9520E-06	3.3620E-06	8.0490E-05	3.8440E-07	
	38	2.5119E+04	1.9953E+04	3.1623E+04	1.2830E-06	2.4350E-06	5.9920E-05	2.4470E-07	
	39	3.9811E+04	3.1623E+04	5.0119E+04	6.4090E-07	1.2420E-06	1.7930E-05	1.1710E-07	
	40	6.3096E+04	5.0119E+04	7.9433E+04	6.4820E-07	1.2280E-06	1.7560E-05	1.1620E-07	
	41	1.0000E+05	7.9433E+04	1.2589E+05	3.8780E-07	8.3930E-07	2.0290E-05	1.0190E-07	
	42	1.5849E+05	1.2589E+05	1.9953E+05	3.1460E-07	6.2580E-07	2.0740E-05	6.9050E-08	
	43	2.5119E+05	1.9953E+05	3.1623E+05	2.3320E-07	3.9840E-07	1.6290E-05	5.5860E-08	
	44	3.9811E+05	3.1623E+05	5.0119E+05	1.5230E-07	2.4400E-07	1.3660E-05	2.1930E-08	
	45	6.3096E+05	5.0119E+05	7.9433E+05	1.8560E-07	2.6300E-07	5.7350E-06	2.1990E-08	
	46	1.0000E+06	7.9433E+05	1.2589E+06	9.7540E-08	1.3860E-07	1.4940E-06	9.3330E-09	
	47	1.5849E+06	1.2589E+06	1.9953E+06	8.6000E-08	1.2280E-07	4.6740E-07	5.7600E-09	
	48	2.5119E+06	1.9953E+06	3.1623E+06	6.6570E-08	1.0270E-07	1.5120E-07	4.9760E-09	
	49	3.9811E+06	3.1623E+06	5.0119E+06	2.5510E-08	3.7620E-08	4.9930E-08	1.9520E-09	
	50	6.3096E+06	5.0119E+06	7.9433E+06	1.6420E-08	1.9940E-08	2.3960E-08	1.1960E-09	
	51	1.0000E+07	7.9433E+06	1.2589E+07	7.3090E-09	9.4750E-09	1.3940E-08	5.5510E-10	
	52	1.5849E+07	1.2589E+07	1.9953E+07	4.7390E-09	6.1590E-09	9.1240E-09	3.3890E-10	
	53	2.5119E+07	1.9953E+07	3.1623E+07	3.8340E-09	5.2330E-09	7.5850E-09	2.2180E-10	
	54	3.9811E+07	3.1623E+07	5.0119E+07	4.1670E-09	5.8450E-09	6.0480E-09	2.8750E-10	
	55	6.3096E+07	5.0119E+07	7.9433E+07	4.3100E-09	5.4760E-09	5.7990E-09	2.2950E-10	
	56	1.0000E+08	7.9433E+07	1.2589E+08	3.0910E-09	4.1020E-09	3.9140E-09	1.9030E-10	
	57	1.5849E+08	1.2589E+08	1.9953E+08	1.5600E-09	1.9630E-09	1.9000E-09	8.8850E-11	
	58	2.5119E+08	1.9953E+08	3.1623E+08	3.8170E-10	4.9900E-10	5.3280E-10	1.8480E-11	
	59	3.9811E+08	3.1623E+08	5.0119E+08	6.0910E-11	8.0170E-11	8.1450E-11	5.0640E-13	
	60	6.3096E+08	5.0119E+08	7.9433E+08	2.9190E-12	4.6160E-12	4.9970E-12	4.1690E-29	
	61	1.0000E+09	7.9433E+08	1.2589E+09	1.9620E-14	3.9900E-13	9.4120E-13	2.6520E-29	
‡total (n/cm <sup>2</sup> PIC-count)					=	1.6897E+00	2.6284E+00	1.6711E+01	2.2768E-01

## APPENDIX E

**THE GROUP VALUES OF THE FLUENCE AND THE DOSE EQUIVQLENT  
FOR ALL FOUR MEASUREMENT POSITIONS AND ALL SOLUTION TYPES**

All the data are given per PIC count !

The neutron energy range covered by the present spectrometric investigations from 1 meV to 1 GeV was divided into 4 energy groups:

- Group 1:** from 1 meV to 0.4 eV
- Group 2:** from 0.4 eV to 10 KeV
- Group 3:** from 10 keV to 10 MeV
- Group 4:** from 10 MeV to 1 GeV

The spectral solutions of different types:

- **Type "61N"** (spectra \*.61N) calculated in Ref. 3, rebinned to match the rest of our data and normalized to one PIC count,
- **Type "53E"** (spectra \*.53E) as presented in Appendix B,
- **Type "61E"** (spectra \*.61E) as presented in Appendix C,
- **Type "61X"** (spectra \*.61X) as presented in Appendix D,

were considered for each of the four measurement positions:

- **CT#6** = CONCRETE TOP POSITION #6
- **CS#2** = CONCRETE SIDE POSITION #2
- **IT#6** = IRON TOP POSITION #6
- **IS#4** = IRON SIDE POSITION #4 (THICK CONCRETE)

and the corresponding group values for neutron fluence and dose equivalent H21, H39 and H60G were calculated and listed in **Table 9** (a and b).

As the solutions of type "61X" are considered to be the *best*, the group values for the other types were recalculated in percent relative to the "61X" values and listed in **Table 10** (a and b).

Table 9a. The group values, absolute and relative to total, of the neutron fluence and dose equivalent H2I, for all types of solutions in all four measurement positions.

File CERN93.APA / Page 1 ( GruVal.EXE ; Energy group limits from File: CERN93.DAG ) ( ALEVRA - PTB 7.22 \* 15.02.94 / 13:47:49 ) Absolute values for the group fluence (in 1/cm<sup>2</sup>)

SPECTRUM	Group limits in eV										TOTAL
	1.000E-04	4.000E-01	1.000E+04	1.000E+07	1.000E+10	1.000E+13	1.000E+16	1.000E+19	1.000E+22	1.000E+25	
CERC76.61N % of total	1.0427E-03 0.08 %	2.0797E-01 16.60 %	4.5779E-01 36.55 %	4.2206E-01 34.09 %	4.6775E-01 38.05 %	5.8578E-01 46.77 %	1.2526E+00 100.00 %	1.000E+09	1.000E+07	1.000E+04	4.1778E-10 100.00 %
C93LCT.53E % of total	2.6836E-01 18.16 %	2.8336E-01 19.18 %	5.0376E-01 34.09 %	4.8754E-01 34.09 %	4.2206E-01 34.09 %	4.2206E-01 34.09 %	1.8059E+00 100.00 %	1.000E+09	1.000E+07	1.000E+04	3.2348E-10 100.00 %
C93-CT.61E % of total	2.7084E-01 15.00 %	2.8083E-01 15.55 %	4.8754E-01 34.09 %	4.8754E-01 34.09 %	4.2206E-01 34.09 %	4.2206E-01 34.09 %	1.8059E+00 100.00 %	1.000E+09	1.000E+07	1.000E+04	5.1931E-10 99.99 %
C93xCT.61X % of total	2.6691E-01 15.80 %	2.8997E-01 17.16 %	5.1567E-01 30.52 %	4.6775E-01 34.09 %	4.2206E-01 34.09 %	4.2206E-01 34.09 %	1.6897E+00 100.00 %	1.000E+09	1.000E+07	1.000E+04	4.4835E-10 100.00 %
CERC82.61N % of total	2.5527E-03 0.12 %	4.6956E-01 22.93 %	8.2112E-01 40.09 %	7.6622E-01 32.92 %	7.6622E-01 32.92 %	7.6622E-01 32.92 %	2.0481E+00 100.00 %	1.000E+09	1.000E+07	1.000E+04	5.8627E-10 99.98 %
C93LCS.53E % of total	5.3293E-01 22.89 %	4.8711E-01 20.92 %	7.6622E-01 32.92 %	7.6622E-01 32.92 %	7.6622E-01 32.92 %	7.6622E-01 32.92 %	2.3286E+00 100.00 %	1.000E+09	1.000E+07	1.000E+04	4.4763E-10 100.00 %
C93-CS.61E % of total	5.5130E-01 19.98 %	4.7190E-01 17.11 %	7.6622E-01 32.92 %	7.6622E-01 32.92 %	7.6622E-01 32.92 %	7.6622E-01 32.92 %	2.7586E+00 100.00 %	1.000E+09	1.000E+07	1.000E+04	6.9911E-10 99.99 %
C93xCS.61X % of total	5.5604E-01 21.16 %	4.6136E-01 17.55 %	8.0178E-01 30.50 %	8.0178E-01 30.50 %	8.0178E-01 30.50 %	8.0178E-01 30.50 %	2.6284E+00 100.00 %	1.000E+09	1.000E+07	1.000E+04	6.1086E-10 99.98 %
CERIT6.61N % of total	1.1632E-03 0.01 %	1.8386E+00 17.49 %	8.0250E+00 76.32 %	8.0250E+00 76.32 %	8.0250E+00 76.32 %	8.0250E+00 76.32 %	1.0514E+01 100.00 %	1.000E+09	1.000E+07	1.000E+04	1.6237E-09 99.99 %
C93LIT.53E % of total	1.6947E-01 1.02 %	3.0815E+00 18.63 %	1.2599E+01 76.18 %	1.2599E+01 76.18 %	1.2599E+01 76.18 %	1.2599E+01 76.18 %	1.6538E+01 100.00 %	1.000E+09	1.000E+07	1.000E+04	2.1635E-09 100.00 %
C93-IT.61E % of total	1.6898E-01 1.00 %	3.0681E+00 18.08 %	1.2556E+01 75.97 %	1.2556E+01 75.97 %	1.2556E+01 75.97 %	1.2556E+01 75.97 %	1.6974E+01 100.00 %	1.000E+09	1.000E+07	1.000E+04	2.4091E-09 100.00 %
C93xIT.61X % of total	1.6894E-01 1.01 %	3.2627E+00 19.52 %	1.2405E+01 74.25 %	1.2405E+01 74.25 %	1.2405E+01 74.25 %	1.2405E+01 74.25 %	1.6711E+01 100.00 %	1.000E+09	1.000E+07	1.000E+04	2.2540E-09 99.99 %
CERIS4.61N % of total	1.2328E-04 0.11 %	2.6185E-02 23.58 %	4.3618E-02 39.28 %	4.3618E-02 39.28 %	4.3618E-02 39.28 %	4.3618E-02 39.28 %	1.1104E+01 100.00 %	1.000E+09	1.000E+07	1.000E+04	3.0969E-11 100.00 %
C93LIS.53E % of total	5.7830E-02 26.37 %	7.3312E-02 33.61 %	6.1525E-02 28.06 %	6.1525E-02 28.06 %	6.1525E-02 28.06 %	6.1525E-02 28.06 %	2.1929E+01 100.00 %	1.000E+09	1.000E+07	1.000E+04	2.5420E-11 100.00 %
C93-IS.61E % of total	5.0377E-02 21.50 %	7.8521E-02 33.51 %	6.0006E-02 25.61 %	6.0006E-02 25.61 %	6.0006E-02 25.61 %	6.0006E-02 25.61 %	2.3433E+01 100.00 %	1.000E+09	1.000E+07	1.000E+04	3.6016E-11 99.99 %
C93xIS.61X % of total	4.9800E-02 21.87 %	7.9357E-02 34.85 %	6.2327E-02 27.37 %	6.2327E-02 27.37 %	6.2327E-02 27.37 %	6.2327E-02 27.37 %	2.2768E+01 100.00 %	1.000E+09	1.000E+07	1.000E+04	3.1625E-11 100.00 %

\*.61N are the calculated ones renormalized to 1 PIC count (multiplied by 2.0E+04)  
The spectra \*.53E are obtained using the response matrix C-1\_00.RES and no preinformation on the spectral distribution  
The spectra \*.61E are obtained using the response matrix C-1\_04.A61 and a limited a priori information on spectra  
The spectra \*.61X are obtained using the response matrix C-1\_04.A61 and the calculated spectra for En > about 10 keV

Table 9b. The group values, absolute and relative to total, of the dose equivalent H39 and H60G, for all types of solutions in all four measurement positions.

File CERN93.APA / Page 2 ( GruVal.EXE ; Energy group limits from File: CERN93.DAG ) ( ALEVRA - PTB 7.22 \* 15.02.94 / 13:47:49 )

Absolute values for the group dose equiv. H39 (in Sv) Absolute values for the group dose equiv. H60G (in Sv)

CERN93.A(P)39(60)		Group Limits in eV										
		1.000E-04 4.000E-01	1.000E-01 1.000E+04	1.000E+04 1.000E+07	1.000E-01 1.000E+07	1.000E+07 1.000E+09	TOTAL	1.000E-04 4.000E-01	1.000E-01 1.000E+04	1.000E+04 1.000E+07	1.000E-01 1.000E+07	1.000E+07 1.000E+09
M e C P o S S i t i o n # 6	CERC16.61N % of total	1.0785E-14 0.00 %	1.6873E-12 0.34 %	1.3542E-10 27.45 %	1.000E+04 1.000E+07	1.000E+07 1.000E+09	4.9266E-10 100.00 %	1.6682E-14 0.00 %	2.5908E-12 0.52 %	1.6913E-10 34.09 %	3.2634E-10 65.38 %	4.9607E-10 100.00 %
	C93LCT.53E % of total	2.3770E-12 0.60 %	2.3776E-12 0.60 %	1.4212E-10 35.86 %	2.4943E-10 62.94 %	3.9630E-10 100.00 %	3.6933E-12 0.89 %	3.6601E-12 0.88 %	1.8396E-10 44.40 %	2.2399E-10 53.82 %	4.1431E-10 100.00 %	
	C93CT.61E % of total	2.4023E-12 0.40 %	2.3465E-12 0.59 %	1.3462E-10 22.17 %	4.6786E-10 77.05 %	6.1002E-10 100.00 %	3.7325E-12 0.61 %	3.6105E-12 0.59 %	1.7456E-10 28.69 %	4.2646E-10 69.04 %	6.0837E-10 100.00 %	
	C93xCT.61X % of total	2.3588E-12 0.45 %	2.3938E-12 0.46 %	1.4626E-10 27.80 %	3.7503E-10 71.29 %	5.2604E-10 100.00 %	3.6653E-12 0.69 %	3.6765E-12 0.69 %	1.8477E-10 34.59 %	3.4212E-10 64.04 %	5.3423E-10 100.00 %	
	CERC2.61N % of total	2.6434E-14 0.00 %	3.8147E-12 0.56 %	2.2289E-10 32.54 %	4.5821E-10 66.90 %	6.8495E-10 99.99 %	4.0888E-14 0.01 %	5.8502E-12 0.83 %	2.4023E-10 35.03 %	4.1800E-10 59.14 %	7.0681E-10 99.99 %	
	C93LCS.53E % of total	4.6989E-12 0.87 %	4.1088E-12 0.76 %	2.1262E-10 39.26 %	3.2019E-10 59.12 %	5.4162E-10 100.00 %	7.3017E-12 1.27 %	6.3286E-12 1.10 %	2.7617E-10 47.94 %	2.8630E-10 49.70 %	5.7609E-10 100.00 %	
M e C P o S S i t i o n # 2	C93CS.61E % of total	4.8927E-12 0.60 %	3.9535E-12 0.49 %	2.0183E-10 24.80 %	6.0331E-10 74.12 %	8.1398E-10 100.00 %	7.6022E-12 0.92 %	6.0850E-12 0.74 %	2.6306E-10 31.82 %	5.4991E-10 66.52 %	8.2666E-10 100.00 %	
	C93xCS.61X % of total	4.9412E-12 0.69 %	3.8337E-12 0.54 %	2.1320E-10 29.87 %	4.9182E-10 68.90 %	7.1380E-10 99.99 %	7.6775E-12 1.05 %	5.8726E-12 0.80 %	2.7169E-10 37.02 %	4.4866E-10 61.13 %	7.3390E-10 99.99 %	
	CER1T6.61N % of total	1.2032E-14 0.00 %	1.3432E-11 0.70 %	1.5067E-09 78.78 %	3.9250E-10 20.52 %	1.9126E-09 99.99 %	1.8610E-14 0.00 %	2.0060E-11 0.78 %	2.1791E-09 85.21 %	3.5812E-10 14.00 %	2.5573E-09 100.00 %	
	C93LIT.53E % of total	1.5209E-12 0.06 %	2.2883E-11 0.89 %	2.1212E-09 82.62 %	4.2186E-10 16.43 %	2.5674E-09 100.00 %	2.3613E-12 0.07 %	3.4227E-11 0.97 %	3.0935E-09 88.01 %	3.8474E-10 10.95 %	3.5148E-09 100.00 %	
	C93IT.61E % of total	1.5143E-12 0.05 %	2.2779E-11 0.81 %	2.0766E-09 73.55 %	7.2086E-10 25.55 %	2.8218E-09 100.00 %	2.3511E-12 0.06 %	3.4069E-11 0.91 %	3.0364E-09 81.41 %	6.5701E-10 17.61 %	3.7298E-09 100.00 %	
	C93xIT.61X % of total	1.5096E-12 0.06 %	2.4110E-11 0.90 %	2.1232E-09 79.29 %	5.2904E-10 19.76 %	2.6779E-09 99.99 %	2.3439E-12 0.06 %	3.5970E-11 0.99 %	3.1075E-09 85.64 %	4.8268E-10 15.30 %	3.6285E-09 100.00 %	
M e I P o S S i t i o n # 4	CERIS4.61N % of total	1.2752E-15 0.00 %	2.0798E-13 0.57 %	1.1527E-11 31.49 %	2.4868E-11 67.94 %	3.6604E-11 100.00 %	1.9724E-15 0.01 %	3.1817E-13 0.85 %	1.4609E-11 38.83 %	2.2692E-11 60.32 %	3.7621E-11 100.00 %	
	C93LIS.53E % of total	5.2101E-13 1.72 %	6.2752E-13 2.07 %	1.3794E-11 45.43 %	1.5420E-11 50.79 %	3.0363E-11 100.00 %	8.0918E-13 2.36 %	9.6813E-13 2.83 %	1.8672E-11 54.49 %	1.3818E-11 40.32 %	3.4267E-11 100.00 %	
	C93IS.61E % of total	4.4068E-13 1.05 %	6.6954E-13 1.60 %	1.3102E-11 31.33 %	2.7605E-11 66.01 %	4.1818E-11 100.00 %	6.8465E-13 1.54 %	1.0326E-12 2.32 %	1.7695E-11 39.69 %	2.5170E-11 56.46 %	4.4583E-11 100.00 %	
	C93xIS.61X % of total	4.3419E-13 1.18 %	6.7236E-13 1.85 %	1.3672E-11 37.25 %	2.1926E-11 59.74 %	3.6705E-11 100.00 %	6.7460E-13 1.70 %	1.0362E-12 2.61 %	1.8042E-11 45.58 %	2.0009E-11 50.32 %	3.9761E-11 100.00 %	

The spectra \*.61N are the calculated ones renormalized to 1 PIC count (multiplied by 2.0E+04)  
 The spectra \*.53E are obtained using the response matrix C-D-90.RES and no preinformation on the spectral distribution  
 The spectra \*.61E are obtained using the response matrix C-I-94.A61 and a limited a priori information on spectra  
 The spectra \*.61X are obtained using the response matrix C-I-94.A61 and the calculated spectra for En > about 10 keV



Table 10a. The group values of the neutron fluence and dose equivalent H21, for all types of solutions relative to the solution of type "61X", in all four measurement positions.

File CERN93.REX / Page 1 ( GruVal.EXE ; Energy group limits from File: CERN93.DAG ) ( ALEVRA - PTB 7.22 \* 15.02.94 / 13:47:49 )

CERN93.RGF ; R21		Percentual dose equivalent H21 relative to *.61X											
		SPECTRUM					Group limits in eV					TOTAL	
M	e	1.000E-04	4.000E-01	1.000E+04	1.000E+07	1.000E+07	1.000E+04	1.000E+07	1.000E+07	1.000E+07	1.000E+07	TOTAL	
		4.000E-01	1.000E+04	1.000E+07	1.000E+07	1.000E+07	1.000E+04	1.000E+07	1.000E+07	1.000E+07	1.000E+07	TOTAL	
M	e	0.39 %	71.72 %	88.78 %	94.92 %	94.92 %	74.13 %	94.92 %	94.92 %	94.92 %	94.92 %	94.92 %	94.92 %
		100.54 %	97.72 %	97.69 %	68.39 %	68.39 %	87.44 %	68.39 %	68.39 %	68.39 %	68.39 %	68.39 %	68.39 %
		101.47 %	96.85 %	94.54 %	124.24 %	124.24 %	106.88 %	124.24 %	124.24 %	124.24 %	124.24 %	124.24 %	124.24 %
		100.00 %	100.00 %	100.00 %	100.00 %	100.00 %	100.00 %	100.00 %	100.00 %	100.00 %	100.00 %	100.00 %	100.00 %
M	e	0.46 %	101.78 %	102.41 %	93.29 %	93.29 %	77.92 %	93.29 %	93.29 %	93.29 %	93.29 %	93.29 %	93.29 %
		95.84 %	105.58 %	95.61 %	66.98 %	66.98 %	88.59 %	66.98 %	66.98 %	66.98 %	66.98 %	66.98 %	66.98 %
		99.15 %	102.28 %	93.09 %	122.22 %	122.22 %	104.95 %	122.22 %	122.22 %	122.22 %	122.22 %	122.22 %	122.22 %
		100.00 %	100.00 %	100.00 %	100.00 %	100.00 %	100.00 %	100.00 %	100.00 %	100.00 %	100.00 %	100.00 %	100.00 %
M	e	0.69 %	56.35 %	64.69 %	74.30 %	74.30 %	62.92 %	74.30 %	74.30 %	74.30 %	74.30 %	74.30 %	74.30 %
		100.31 %	94.45 %	101.56 %	78.63 %	78.63 %	98.96 %	78.63 %	78.63 %	78.63 %	78.63 %	78.63 %	78.63 %
		100.02 %	94.04 %	101.22 %	135.00 %	135.00 %	101.57 %	135.00 %	135.00 %	135.00 %	135.00 %	135.00 %	135.00 %
		100.00 %	100.00 %	100.00 %	100.00 %	100.00 %	100.00 %	100.00 %	100.00 %	100.00 %	100.00 %	100.00 %	100.00 %
M	e	0.25 %	33.00 %	69.98 %	113.56 %	113.56 %	48.77 %	113.56 %	113.56 %	113.56 %	113.56 %	113.56 %	113.56 %
		116.12 %	92.89 %	98.71 %	72.44 %	72.44 %	96.32 %	72.44 %	72.44 %	72.44 %	72.44 %	72.44 %	72.44 %
		101.16 %	98.95 %	96.28 %	125.48 %	125.48 %	102.92 %	125.48 %	125.48 %	125.48 %	125.48 %	125.48 %	125.48 %
		100.00 %	100.00 %	100.00 %	100.00 %	100.00 %	100.00 %	100.00 %	100.00 %	100.00 %	100.00 %	100.00 %	100.00 %

The spectra \*.61N are the calculated ones renormalized to 1 PIC count (multiplied by 2.0E+04)  
 The spectra \*.53E are obtained using the response matrix C-D\_90.RES and no preinformation on the spectral distribution  
 The spectra \*.61E are obtained using the response matrix C-1\_94.A61 and a limited a priori information on spectra  
 The spectra \*.61X are obtained using the response matrix C-1\_94.A61 and the calculated spectra for En > about 10 keV

Table 10b. The group values of the dose equivalent H39 and H60G, for all types of solutions relative to the solution of type "61X", in all four measurement positions.

File CERN93.REX / Page 2 ( GruVal.EXE ; Energy group limits from File: CERN93.DAG ) ( ALEVRA - PTB 7.22 \* 15.02.94 / 13:47:49 )

Percentual dose equivalent H39 relative to \*.61X

Percentual dose equivalent H60G relative to \*.61X

CERN93.R39 ; R60		Group limits in eV						Group limits in eV					
		1.000E-04 4.000E-01	4.000E-01 1.000E+04	1.000E+04 1.000E+07	1.000E+07 1.000E+09	TOTAL	1.000E-04 4.000E-01	4.000E-01 1.000E+04	1.000E+04 1.000E+07	1.000E+07 1.000E+09	TOTAL		
M	CERT6.61N	0.46 %	70.49 %	92.59 %	94.81 %	93.65 %	0.46 %	70.47 %	91.54 %	94.80 %	92.86 %		
a	C93LCT.53E	100.77 %	99.32 %	97.17 %	66.51 %	75.34 %	100.76 %	99.55 %	99.56 %	65.18 %	77.55 %		
S	C93-CT.61E	101.84 %	98.02 %	92.04 %	124.75 %	115.43 %	101.83 %	98.20 %	94.47 %	124.65 %	113.88 %		
T	C93xCT.61X	100.00 %	100.00 %	100.00 %	100.00 %	100.00 %	100.00 %	100.00 %	100.00 %	100.00 %	100.00 %		
P	CERCS2.61N	0.53 %	99.50 %	104.55 %	93.17 %	95.96 %	0.53 %	99.62 %	104.13 %	93.17 %	96.31 %		
o	C93LCS.53E	95.10 %	107.18 %	99.73 %	65.10 %	75.88 %	95.11 %	107.76 %	101.65 %	63.81 %	78.50 %		
6	C93-CS.61E	99.02 %	103.12 %	94.67 %	122.67 %	114.03 %	99.02 %	103.62 %	96.82 %	122.57 %	112.64 %		
s	C93xCS.61X	100.00 %	100.00 %	100.00 %	100.00 %	100.00 %	100.00 %	100.00 %	100.00 %	100.00 %	100.00 %		
M	CERT16.61N	0.80 %	55.71 %	70.96 %	74.19 %	71.42 %	0.79 %	55.75 %	70.12 %	74.19 %	70.48 %		
a	C93LIT.53E	100.75 %	94.91 %	99.91 %	79.74 %	95.87 %	100.74 %	95.13 %	99.55 %	79.71 %	96.87 %		
S	C93-IT.61E	100.31 %	94.48 %	97.81 %	136.26 %	105.37 %	100.31 %	94.69 %	97.71 %	136.12 %	102.79 %		
T	C93xIT.61X	100.00 %	100.00 %	100.00 %	100.00 %	100.00 %	100.00 %	100.00 %	100.00 %	100.00 %	100.00 %		
P	CER154.61N	0.29 %	30.93 %	84.31 %	113.42 %	99.72 %	0.29 %	30.71 %	80.97 %	113.41 %	94.62 %		
o	C93LIS.53E	120.00 %	93.33 %	100.89 %	70.33 %	82.72 %	119.95 %	93.43 %	103.49 %	69.06 %	86.18 %		
6	C93-IS.61E	101.49 %	99.58 %	95.83 %	125.90 %	113.93 %	101.49 %	99.65 %	98.08 %	125.79 %	112.13 %		
s	C93xIS.61X	100.00 %	100.00 %	100.00 %	100.00 %	100.00 %	100.00 %	100.00 %	100.00 %	100.00 %	100.00 %		

The spectra \*.61N are the calculated ones renormalized to 1 PIC count (multiplied by 2.0E+04)  
 The spectra \*.53E are obtained using the response matrix C-D\_90.RES and no preinformation on the spectral distribution  
 The spectra \*.61E are obtained using the response matrix C-1\_94.A61 and a limited a priori information on spectra  
 The spectra \*.61X are obtained using the response matrix C-1\_94.A61 and the calculated spectra for En > about 10 keV



## PTB-Berichte der Serie N (Neutronenphysik)

- N-1: G. Börker, R. Böttger, H. J. Brede, H. Klein u. a.:  
**Elastic and Inelastic Differential Neutron Scattering Cross Sections of Oxygen between 6 and 15 MeV.**  
120 S., 6 Abb., 57 Tab., ISBN 3-88314-906-3, 1989, DM 32,50
- N-2: B. W. Bauer, W. G. Alberts, M. Luszig-Bhardra,  
B. R. L. Siebert:  
**Experimental Investigation into the Influence of Neutron Energy, Angle of Incidence and Phantom Shape on the Response of Individual Neutron Dosimeters: Detailed Analysis of Results for the Albedo Neutron Dosimeter in Use at the PTB.**  
54 S., 21 Abb., ISBN 3-89429-005-6, 1990, DM 20,50
- N-3: H. Schumny:  
**Personal Computers for Data Acquisition and Measurement, Standards interfaces, State of the Art, Trends, Applications.**  
66 S., 24 Abb., 5 Tab., ISBN 3-89429-009-9, 1990, DM 23,50
- N-4: D. R. Schlegel-Bickmann, H. J. Brede, S. Guldbakke u. a.:  
**Measurement of  $k_p$ -Values of Argon-Filled Magnesium Ionisation Chambers.**  
76 S., zahlr. Tab., ISBN 3-89429-063-3, 1990, DM 26,00
- N-5: B. W. Bauer, B. R. L. Siebert, W. G. Alberts u. a.:  
**Experimental Investigation into the Influence of Neutron Energy, Angle of Incidence and Phantom Shape on the Response of Individual Neutron Dosimeters: Experimental Procedure and Summary of Results.**  
36 S., 5 Abb., 10 Tab., ISBN 3-89429-072-2, 1990, DM 17,00
- N-6: B. R. L. Siebert, W. G. Alberts, B. W. Bauer:  
**Computational Study of Phantoms for Individual Neutron Dosimetry.**  
40 S., 20 Abb., 10 Tab., ISBN 3-89429-075-7, 1990, DM 17,50
- N-7: D. Schmidt, R. Böttger, H. Klein, R. Nolte:  
**Investigation of the  ${}^9\text{Be}(\alpha, n) {}^{12}\text{C}$  Reaction. I: Experimental Procedure and Uncertainties.**  
42 S., 22 Abb., ISBN 3-89429-176-1, 1992, DM 20,00
- N-8: D. Schmidt, R. Böttger, H. Klein, R. Nolte:  
**Investigation of the  ${}^9\text{Be}(\alpha, n) {}^{12}\text{C}$  Reaction. II. Differential Cross Sections for  $E_\alpha = 7.02 - 15.70$  MeV and  $E_n({}^{12}\text{C}) = 0.0, 4.439, 7.654, 9.641, 10.84, 11.83$  and  $12.71$  MeV.**  
96 S., 44 Abb., 3 Tab., ISBN 3-89429-177-X, 1992, DM 32,00
- N-9: R. Nolte, H. Schuhmacher, H. J. Brede, U. J. Schrewe:  
**Neutron Spectrometry with Liquid Scintillation Detectors at Neutron Energies between 20 MeV and 70 MeV: A Status Report.**  
58 S., 17 Abb., ISBN 3-89429-328-4, 1993, DM 23,50
- N-10: W. G. Alberts (Hrsg.):  
**Investigation of Individual Neutron Monitors on the Basis of Etched-track Detectors: The 1990 EURADOS-CENDOS Exercise.**  
136 S., ISBN 3-89429-198-2, 1992, DM 36,00
- N-11: K. Weise, W. Wöger:  
**Eine Bayessche Theorie der Meßunsicherheit.**  
34 S., ISBN 3-89429-227-X, 1992, DM 18,50
- N-12: R. A. Hollnagel:  
**Comparison of the Effective Dose, E, and the Effective Dose Equivalent, H<sub>E</sub>, from Neutron Irradiation with Special Regard to the Dose from Induced Photons.**  
54 S., 15 Abb., ISBN 3-89429-261-X, 1992, DM 22,50
- N-13: H. Schuhmacher, U. J. Schrewe:  
**Dose Equivalent Measurements on Board Civil Aircraft.**  
42 S., 14 Abb., 5 Tab., ISBN 3-89429-306-3, 1993, DM 20,00
- N-14: D. Schmidt, B. R. L. Siebert:  
**Monte Carlo Simulation of Fast Neutron Scattering Experiments Including DD-Breakup Neutrons.**  
48 S., 34 Abb., ISBN 3-89429-332-2, 1993, DM 22,50
- N-15: W. G. Alberts, H. Kluge:  
**PTB-Vergleichsmessungen an Personendosimetern für Neutronenstrahlung.**  
40 S., 28 Abb., 12 Tab., ISBN 3-89429-352-7, 1993, DM 20,50
- N-16: M. Weyrauch, K. Weise:  
**Untersuchung der Unsicherheiten bei der Messung mit Thermolumineszenz-Dosimetern.**  
28 S., 3 Abb., ISBN 3-89429-374-8, 1993, DM 18,00
- N-17: P. Mikula, V. Wagner, R. Scherm:  
**On the focusing in neutron diffraction by elastically bent perfect crystals.**  
34 S., 13 Abb., ISBN 3-89429-478-7, 1994, DM 19,50
- N-18: D. Schmidt, Xia Haihong:  
**Neutron Production by Deuteron Breakup on  ${}^4\text{He}$ .**  
ca. 39 S., 15 Abb., 2 Tab., ISBN 3-89429-536-8, 1994, ca. DM 20,50
- N-19: M. Matzke:  
**Unfolding of Pulse Height Spectra: The HEPRO Program System.**  
ca. 73 S., ISBN 3-89429-543-0, 1994, ca. DM 28,00
- N-20: D. Schmidt, W. Mannhart, H. Klein, R. Nolte:  
**Neutron Scattering on Natural Iron at Incident Energies between 9.4 and 15.2 MeV.**  
ca. 157 S., zahlr. Abb. und Tab., ISBN 3-89429-552-X, 1994, ca. DM 40,00
- N-21: B. Wiegel, A. V. Alevra, B. R. L. Siebert:  
**Calculations of the Response Functions of Bonner Spheres with a Spherical  ${}^3\text{He}$  Proportional Counter Using a Realistic Detector Model.**  
ca. 92 S., zahlr. Abb., ISBN 3-89429-563-5, 1994, ca. DM 31,00
- N-22: A. V. Alevra, H. Klein, U. Schrewe:  
**Measurements with the PTB Bonner Sphere Spectrometer in High-Energy Neutron Calibration Fields at CERN.**  
ca. 47 S., zahlr. Tab., ISBN 3-89429-573-2, 1994, ca. DM 22,00

